applied sciences

MDPI

Article

Integrated Geotechnical Analysis of Allophanic Volcanic Ash Soils: SDMT and Laboratory Perspectives

Eddy Fernando Sanchez [1,*], Jorge Albuja-Sánchez [1,2] and Maritza Córdova [1]

[1] Faculty of Engineering, Laboratory of Materials Resistance, Soil Mechanics, Pavements and Geotechnics, Pontificia Universidad Católica del Ecuador (PUCE), Quito 170143, Ecuador; jdalbuja@puce.edu.ec (J.A.-S.); mcordova001@puce.edu.ec (M.C.)

[2] Multidisciplinary Engineering Research Hub, International Faculty of Innovation PUCE-Icam, Pontificia Universidad Católica del Ecuador (PUCE), Quito 170143, Ecuador

* Correspondence: efsanchez@puce.edu.ec

Abstract: The geological study area is volcano-tectonic in nature. Microscopic observations and mineralogical analyses revealed the presence of allophane and diatom clusters whose mineral compositions coincided with weathered andesites and dacites. Edometric consolidation tests showed a high porosity and a reduction in the void ratio by up to five times. These are highly compressible soils with a Cc/Cs ratio of 12 to 15 and a specific gravity (Gs) of 2.4. Low initial bulk density (1.10 Mg/m^3), high plasticity, and SUCS (OH) classification are typical of soft soils, with an effective friction angle (ϕ'_{CD}) of 25.5° to 30° and effective cohesion (c'_{CD}) of 11.90 to 47.27 KPa. The shear wave velocity for the first 10 m (Vs10) on average ranged from 78 m/s to 120 m/s, whereas that for the first 30 m (Vs30) was 169 m/s. The permeability, which was calculated indirectly, was between 2×10^{-7} and 3×10^{-8} m/s. With an organic matter content between 5% and 25%, the Caupicho soil is an organic mineral sediment that is not considered peat (non-peat). The results of this study serve as a basis for future analyses of soil dynamics, bearing capacity, and consolidation settlements in the medium and long term in an area of high urban growth in southern Quito, Ecuador.

Keywords: allophanic soils; diatomaceous soils; Marchetti's dilatometer test; physical–mechanical–geotechnical characterization of soils

Academic Editor: Tiago Filipe da Silva Miranda

Received: 28 November 2024
Revised: 19 January 2025
Accepted: 26 January 2025
Published: 29 January 2025

Citation: Sanchez, E.F.; Albuja-Sánchez, J.; Córdova, M. Integrated Geotechnical Analysis of Allophanic Volcanic Ash Soils: SDMT and Laboratory Perspectives. *Appl. Sci.* **2025**, *15*, 1386. https://doi.org/10.3390/app15031386

1. Introduction

Masonry cracks in housing and enclosures in the Caupicho and Garrochal neighborhoods in a volcano-tectonic zone [1] and soft soils with lacustrine evidence motivated this study.

The current research includes thin film mineralogy, Rx diffraction, scanning electron microscopy (SEM), triaxial CU, and permeability research not previously performed, obtaining in situ geotechnical parameters by the Marchetti SDMT test at 10 m depth (soil specific gravity (Ɣ), material index (ID), lateral soil pressure coefficient (Ko), ratio between preconsolidation pressure σc and present effective vertical pressure σ'o (OCR), angle of internal friction (ϕ), cohesion of undrained unconsolidated soil (Cu), horizontal permeability (Kh), and seismic wave velocity (Vs)) and physical–mechanical geotechnical characterization (granulometry, Atterberg limits, specific gravity, moisture content, organic content, oedometric consolidation test, and drained consolidated triaxial test). All these tests were carried out to understand the geological, chemical, mineralogical history, and

physical–mechanical characteristics applicable to engineering studies in soft soils of the Caupicho sector, south of Quito. This study was compared with others carried out in the area by Mayanquer [2], Albuja [3,4], Peñafiel [5], and Seismic Quito [6], finding valuable correlations.

The structural geology in the study area indicates anticlines and a reverse geological fault generated by tectonic compression between the valley of Tumbaco and the valley of Quito. The soils formed were of volcanic origin from sources such as Atacazo and El Corazon [7–9]. The allophanes found in soils of volcanic origin, or andosols, with a diameter of 3–5 nm, are composed of silica tetrahedra (Si) and aluminum octahedra (Al) [10]. In Ecuador, andosols are distributed in the north-central highlands in high and humid zones [10]. Mizota, 1982 [11], stated that the coexistence of diatoms with allophanes in andosols may indicate an early stage of soil development. Porous particles (allophane, imogolite, diatoms, plagioclase, and volcanic glass) largely explain the high porosity of the volcanic ash, with maximum void ratios of approximately 5. Guojun, 2019 [12], believed that the reasons for the resistance to liquefaction lie largely in the nature of the allophane particles (which form the "fines"), in particular, the surface properties of the allophane particles and the strong electrostatic bonding between them. Sludges and mires depend on the amount of organic matter to be considered as peat [13,14]. Diatomaceous soils are significantly more compressible than fine soils with a similar geotechnical classification [15].

Owing to the accelerated urbanization in southern Quito, additional geotechnical studies are required to evaluate the bearing capacity of the soil, liquefaction, and consolidation settlement, among others.

2. Materials and Methods

2.1. Location

Figure 1 shows the perforations Caupicho1 (774640; 9962997), Caupicho2 (774434; 9962779), and Caupicho3 (774177; 9963435), located to the northeast of the previous studies of Mayanquer (774589; 9962384) [2], Albuja (774642; 9962470) [3,4], and Peñafiel (774506; 9962779) [5], P4-SQ, P5-SQ [6].

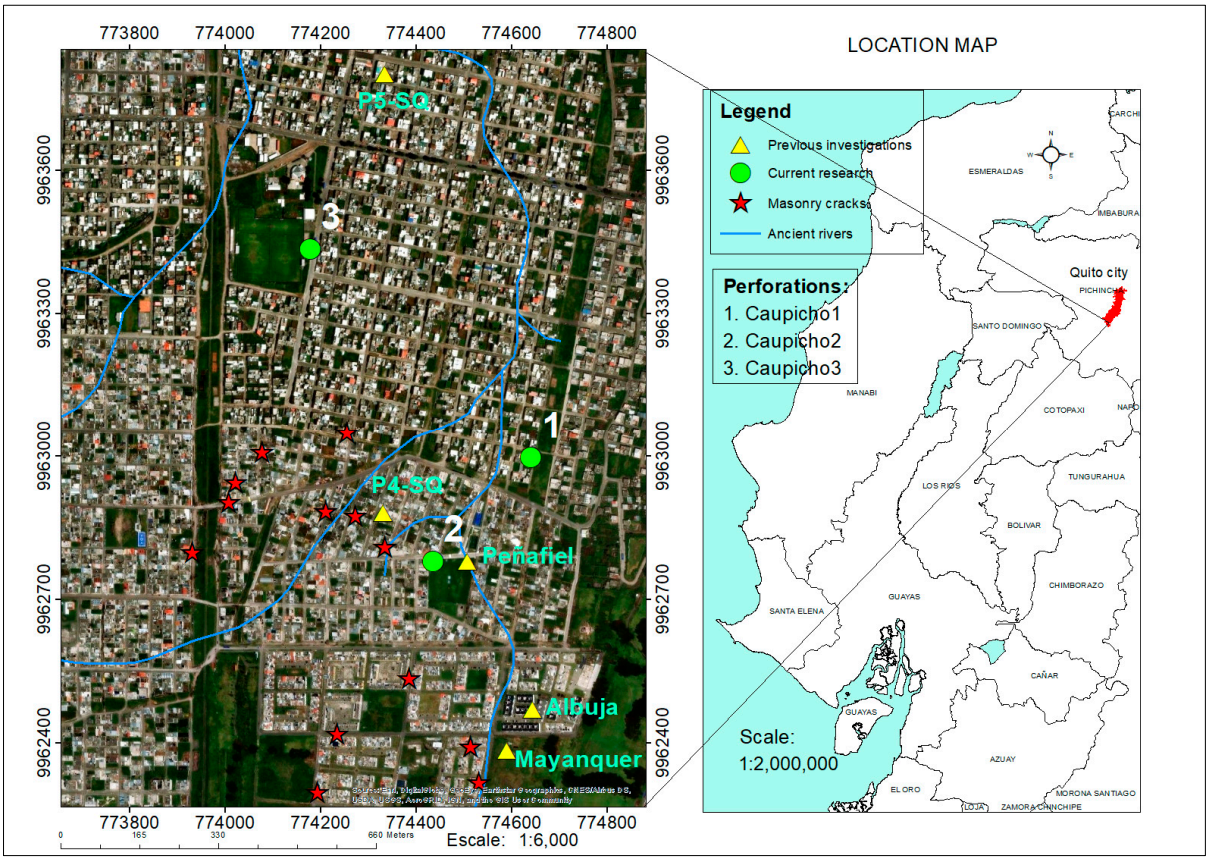

Figure 1. Caupicho study area (coordinate system: Datum WGS 84 – Projection UTM Zone 17 S) [16].

A brief field study revealed cracks in the masonry of houses and enclosures (Figure 2). The geographical location of the affected infrastructure is shown in Figure 1 (masonry cracks).

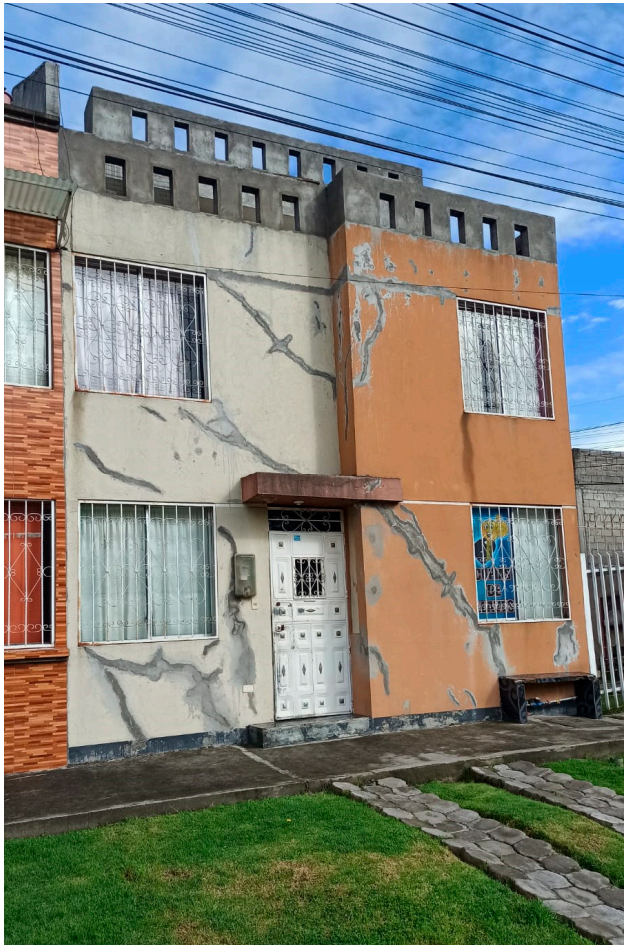

(**a**)

(**b**)

(**c**)

(**d**)

(**e**)

(**f**)

Figure 2. (**a**) Repaired cracks in masonry; (**b**) unrepaired masonry cracks; (**c**) cracks between masonry and floor beam; (**d**) cracks in masonry and dampness in walls owing to capillarity; (**e**) crack in enclosure attached to a three-story house and capillary dampness; (**f**) crack in the enclosure and sidewalk.

a. Climatology

In Tables 1 and 2 we have the climatic variables obtained from the Santa Catalina meteorological station located approximately 3.4 km south of Caupicho using the FAO ClimWat and CropWat software [17,18].

Table 1. Climate variables. Santa Catalina Weather Station. Latitude: 0.36 S, longitude: 78.55 W, height: 3058 m [17,18].

Month	Min Temp	Max Temp	Humidity	Wind	Insolation	Rad	ETo
	°C	°C	%	km/day	hours	MJ/m²/day	mm/day
January	5.90	18.10	79	181	4.00	15.20	2.84
February	6.20	17.60	79	190	3.50	14.80	2.78
March	6.40	17.60	80	181	3.30	14.60	2.74
April	6.40	17.60	81	181	2.80	13.50	2.56
May	6.30	17.90	87	181	4.20	14.80	2.55
June	5.30	17.70	81	216	4.50	14.50	2.64
July	4.90	18.20	70	268	4.70	15.10	3.09
August	4.60	18.60	69	259	4.80	16.00	3.30
September	4.80	18.60	72	242	4.40	16.10	3.22
October	5.30	18.20	78	181	3.60	14.90	2.86
November	5.60	18.00	79	173	3.90	14.90	2.79
December	5.80	18.10	78	181	4.10	15.10	2.83
Average	5.60	18.00	78	203	4.00	15.00	2.85

Table 2. Monthly precipitation. Santa Catalina Weather Station. Latitude: 0.36 S, longitude: 78.55 W, height: 3058 m [17,18].

Month	January	February	March	April	May	June	July	August	September	October	November	December	Total
Precipitation (mm)	132	157	173	192	140	68	31	40	86	141	142	121	1423

b. Geology

The Carcacha volcanic edifice has an age of 1.29 Ma. The Atacazo caldera volcano has an age of 84–220 Ka (domes and andesitic lava flows) [8,9]. Approximately 15 km south of Atacazo, another volcano, Corazón, has experienced pyroclastic eruptions over the last 20,000 years [9]. The domes La Viudita, Gallo Cantana, and Ninahuilca Chico I and II are formed by dacites containing plagioclase, amphibole, orthopyroxene, magnetite, and biotite. Arenal I and II were formed by andesites and dacites containing plagioclase, amphibole, orthopyroxene, and magnetite (Figure 3) [8,9]. Structurally, to the east of the study area, there is an anticlinal and geological fault parallel to the Machángara River [1].

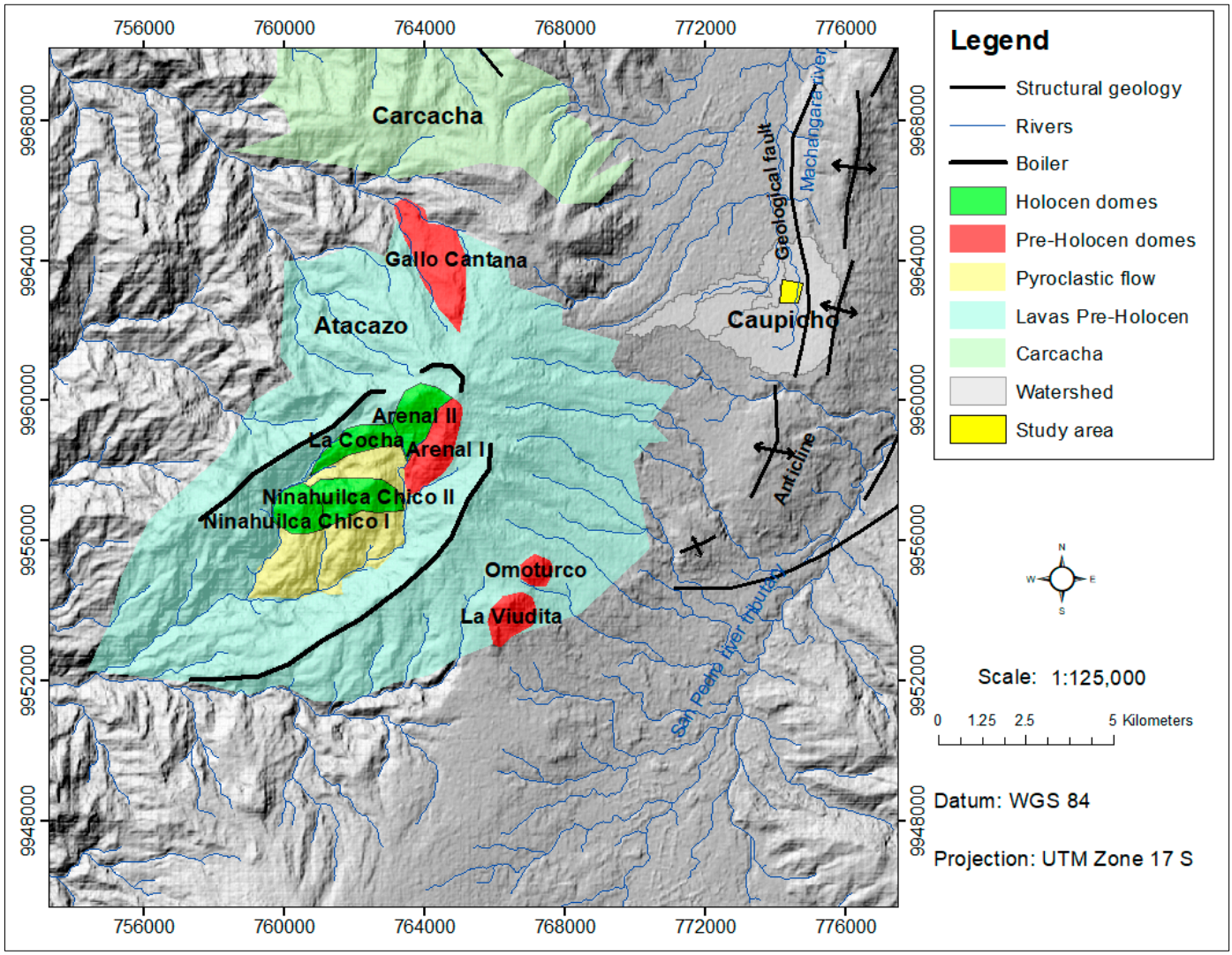

Figure 3. Atacazo–Ninahuilca geological map (coordinate system: Datum WGS 84 – Projection UTM Zone 17 S) [7–9].

c. Hydrology

With the information from the watersheds contributing to the Caupicho area (Figure 2), the soil texture [19,20] and runoff coefficient from 0.11 to 0.16 were identified (Table 3).

Table 3. Calculation of the surface runoff coefficient for Caupicho.

Soil Texture	Area (Ha)	%	Runoff Coefficient (Ce)		%/100 x Ce	
			Minimum	Maximum		
Urban areas	4.98	1.00	0.30	0.50	0.00	0.00
Clayey	51.96	7.00	0.18	0.22	0.01	0.01
Sandy loam (fine to coarse)	386.15	50.00	0.10	0.15	0.05	0.08
Silt loam	326.34	42.00	0.10	0.15	0.04	0.06
Total	769.42	100.00			0.11	0.16

Using the rational method, the runoff coefficient, length of the river (L), slope of the basin (S), time of concentration (tc) (1) [20], and INAMHI data [21], a maximum surface runoff flow of 14.22 cm for a return period of 100 years was calculated (Table 4).

$$tc = 0.000325 \frac{L^{0.77}}{S^{0.385}} \quad (1)$$

Table 4. Calculation of the maximum flow for a 100-year return period in Caupicho.

Basin Area	Channel Length (L)	River Slope (S)	Return Time	Runoff Coefficient (Ce)	Concentration Time (tc)	Daily Intensity (Idtr)	Maximum Intensity of Rain (Itr)	Maximum Flow
Km²	m	m/m	years		minutes	mm/hr	mm/hr	cms
5.13	4281.00	0.03	100.00	0.16	47.06	3.30	62.35	14.22

Table 5 shows the maximum flow calculated for different return periods.

Table 5. Calculation of maximum flow for different return periods.

Return Period	Daily Intensity (Idtr)	Maximum Intensity of Rain (Itr)	Maximum Flow
Year	mm/hr	mm/hr	cm
2	1.80	34.00	7.75
5	2.00	37.79	8.62
10	2.30	43.46	9.91
25	2.60	49.12	11.20
50	3.00	56.68	12.92
100	3.30	62.35	14.22

2.2. In Situ Tests

In Table 6 we have the parameters obtained with SDMT in the Caupicho1, 2, and 3 boreholes: soil specific gravity (Y), material index (I_D), lateral soil pressure coefficient (Ko), ratio between the preconsolidation pressure σ'c and the present effective vertical pressure σ'o (OCR), internal friction angle (ϕ), cohesion of unconsolidated undrained soil (Cu), horizontal permeability (Kh), and seismic wave velocity (Vs).

Table 6. SDMT Parameters.

In Situ Test	Parameters	Reference
SDMT	Y, I_D, Ko, OCR, ϕ, Cu, Kh, Vs	[22,23]

2.3. Specimen Preparation

Laboratory tests were conducted at PUCE after obtaining Shelby tubes at a depth of 10 m in Caupicho1. Prior to the test, the unaltered samples were kept in a humid room to preserve their natural humidity.

2.4. Laboratory Tests

The laboratory test results are presented in Table 7.

Table 7. Laboratory tests.

Laboratory Test	Parameters	Reference
Thin-section mineralogy	Mineral content	[24]
Rx diffraction	Mineral content	[25]
Scanning electron microscope (SEM)	Chemical form	[26]
Moisture content	w (%)	[27]
Atterberg limits	Ll, Lp, Ip (%)	[28]
Material finer than 75 μm	Fines (%)	[29]
USCS classification	Soil classification	[30]
Ash and organic content	Ash content, organic material	[31]
Unit weight	Y	[32]
Triaxial CU	c', ϕ'	[33]

Oedometric consolidation	Cc, Cs, Cv, Kv	[34]

2.4.1. Thin-Film Mineralogy

Thin-film mineralogy is a technique used for the analysis of rocks and minerals using optical microscopy. It consists of preparing a very thin section of the sample, usually approximately 30 μm thick, which is placed on a glass slide. This thin slide is sufficiently transparent to allow polarized light to pass through. We worked on an unaltered sample of Caupicho previously dried in open air, applied a special epoxy, and prepared thin films. The test was conducted at the Faculty of Geology and Petroleum, Department of Geology, National Polytechnic School [24].

2.4.2. Rx Diffraction

Prior to the test, the soil was calcined in a SNOL muffle for two hours at a controlled rising temperature until it reached 650 degrees Celsius [6]. The compounds with defined crystallization present in the sample were determined using the Diffractometer D8 ADVANCE and the Diffrac Plus program (EVA and TOPAS) for qualification and semi-quantification. The test was conducted at the Department of Extractive Metallurgy, National Polytechnic School [25].

2.4.3. Scanning Electron Microscope (SEM)

All morphology and elemental chemistry assays were performed using Dutch PHENOM PRO-X equipment with the serial number MVE0231871255, located at the Faculty of Exact and Natural Sciences, School of Chemical Sciences, Laboratory 007 of the Fundamental and Applied Electrochemistry Group GEFA, Pontificia Universidad Católica del Ecuador. An accelerating voltage of 15 kV was used at magnifications of 810×, 410×, and 400× [26].

2.4.4. Physical–Geotechnical Characterization of Caupicho

The physical–geotechnical characterization of soil involves in situ sample extraction, transport, and storage in a room that maintains humidity, as well as laboratory analysis of grain size, Atterberg limits, specific gravity, moisture content, and organic content.

2.4.5. Mechanical–Geotechnical Characterization of Caupicho

The mechanical–geotechnical characterization of soils by triaxial and consolidation testing involves evaluating their strength and deformability under controlled conditions. These tests are fundamental for understanding the behavior of soils under different loading and confining conditions, which is crucial for the design and construction of geotechnical structures. The consolidation test measures how the soil compresses and expels water under an applied load over time. This test is essential for evaluating the settlement of the soils under these structures. In the triaxial consolidated–drained (CD) test, the sample was fully consolidated before axial loading was applied, allowing drainage during the test.

3. Results

3.1. In Situ Test Result

The in situ tests were carried out at three locations: Caupicho1, 2, and 3. A Marchetti dilatometer (DMT) was used in this study.

3.1.1. Dilatometer Result

The material index I_D was used to determine the soil type using DMT, as listed in Table 8 [35].

Table 8. Soil type and material index (I_D) for cohesive and granular soils.

	Soil Type	Material Index (I_D)	
Organic soils and cohesive soils	Peat/Sensitive clays	<0.10	
	Clay	0.10	0.35
	Silty clay	0.35	0.60
	Clayey silt	0.60	0.90
	Silt	0.90	1.20
	Sandy silt	1.20	1.80
Non-cohesive soils	Silty sand	1.80	3.30
	Sand	>3.30	

The percentages of soil types in the three in situ boreholes are listed in Table 9.

Table 9. Soil type in percentages for Caupicho.

Soil	Caupicho1	Caupicho2	Caupicho3
	%	%	%
MUD *	52.63	68.42	0.00
Clay	0.00	1.75	0.00
Silty clay	10.53	12.28	35.71
Clayey silt	5.26	3.51	16.67
Silt	8.77	7.02	4.76
Sandy silt	7.02	3.51	14.29
Silty sand	8.77	0.00	14.29
Sandy silt	7.02	3.51	14.29
Total	100.00	100.00	100.00

* Silt or clay mixed with water.

The geotechnical characterization of soils using in situ DMT tests is shown in Figure 4.

Figure 5 shows the type of soil based on the dilatometer modulus (E_D) and material index (I_D), with a considerable percentage of soil classified as muck/peat.

Table 10 shows the muck/peat percentages obtained using the E_D–I_D parameters, as shown in Figure 5. Caupicho1 had 56.6% muck/peat, and Caupicho2 had 69.6% muck/peat. Caupicho3 does not present muck/peat data.

Table 10. Marchetti's nomogram analysis. Muck/peat determination.

Muck/Peat	Caupicho1	Caupicho2	Caupicho3
	%	%	%
Yes	56.6	69.6	0.0
No	43.4	30.4	100.0
Total	100.0	100.0	100.0

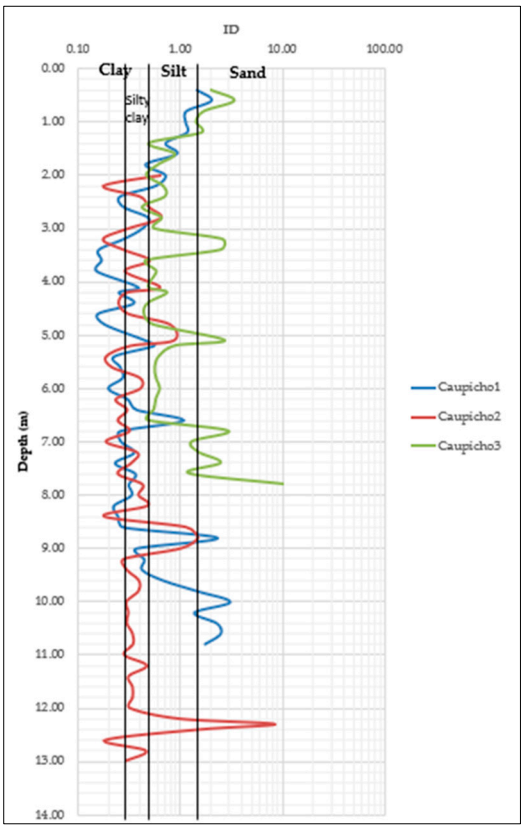
ID
0.10
1.00
10.00
100.00
Clay
Silt
Sand
Silty clay
Depth (m)
0.00
1.00
2.00
3.00
4.00
5.00
6.00
7.00
8.00
9.00
10.00
11.00
12.00
13.00
14.00
Caupicho1
Caupicho2
Caupicho3

(**a**)

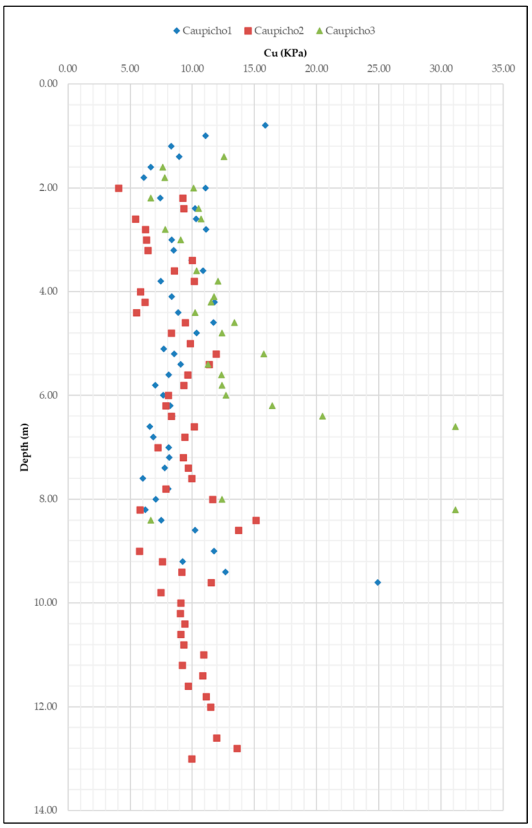
Caupicho1
Caupicho2
Caupicho3
Cu (KPa)
0.00
5.00
10.00
15.00
20.00
25.00
30.00
35.00
Depth (m)
0.00
2.00
4.00
6.00
8.00
10.00
12.00
14.00

(**b**)

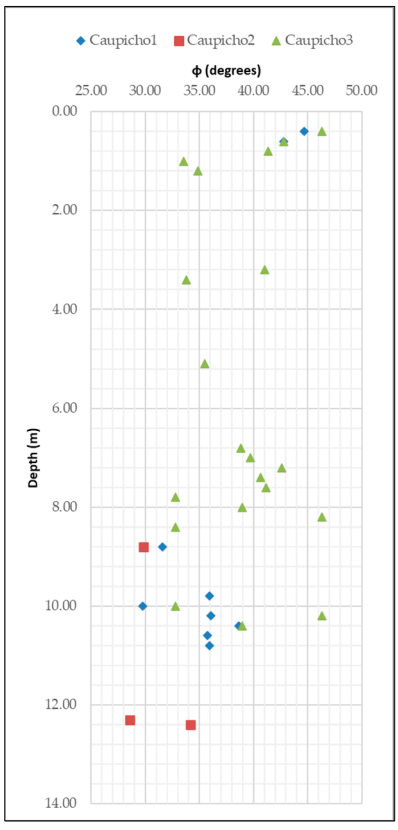
Caupicho1
Caupicho2
Caupicho3
ϕ (degrees)
25.00
30.00
35.00
40.00
45.00
50.00
Depth (m)
0.00
2.00
4.00
6.00
8.00
10.00
12.00
14.00

(**c**)

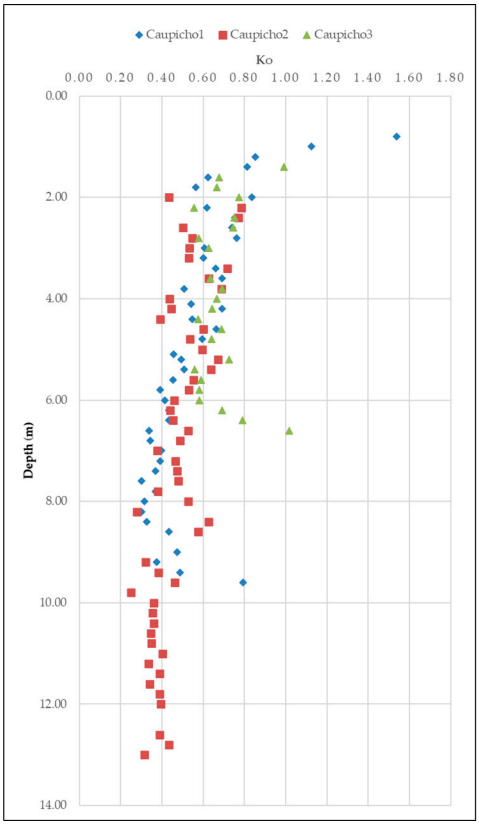
Caupicho1
Caupicho2
Caupicho3
Ko
0.00
0.20
0.40
0.60
0.80
1.00
1.20
1.40
1.60
1.80
Depth (m)
0.00
2.00
4.00
6.00
8.00
10.00
12.00
14.00

(**d**)

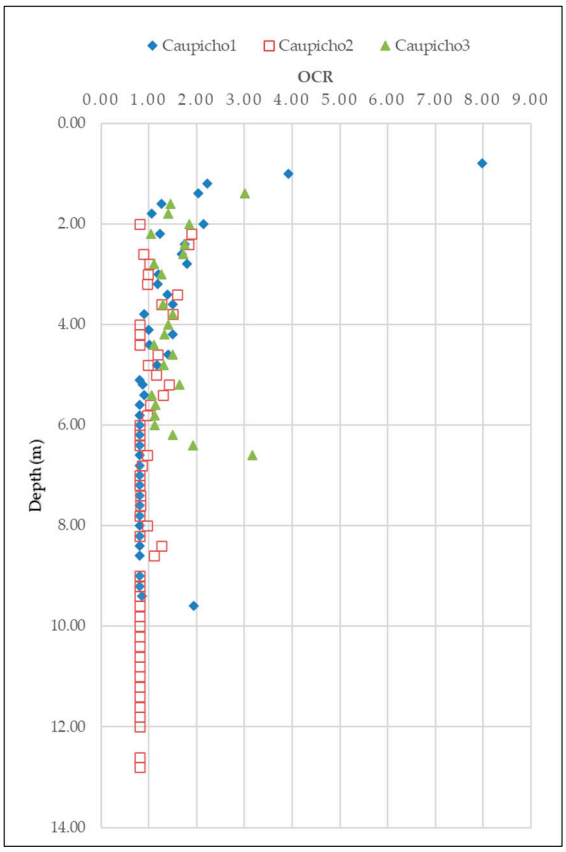

(**e**)

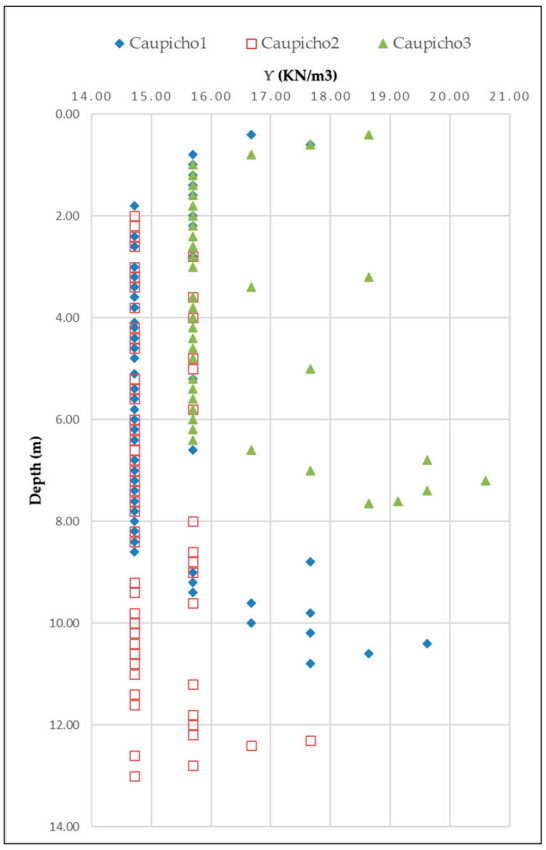

(**f**)

Figure 4. Geotechnical parameters of Caupicho in relation to depth, using the Marchetti dilatometer, listed as: (**a**) material index (I_D); (**b**) cohesion of unconsolidated undrained soil (Cu); (**c**) angle of internal friction (ϕ); (**d**) coefficient of lateral soil pressure (Ko); (**e**) relationship between preconsolidation pressure σc and the effective vertical pressure present σ'o (OCR); and (**f**) specific weight of soil (Y).

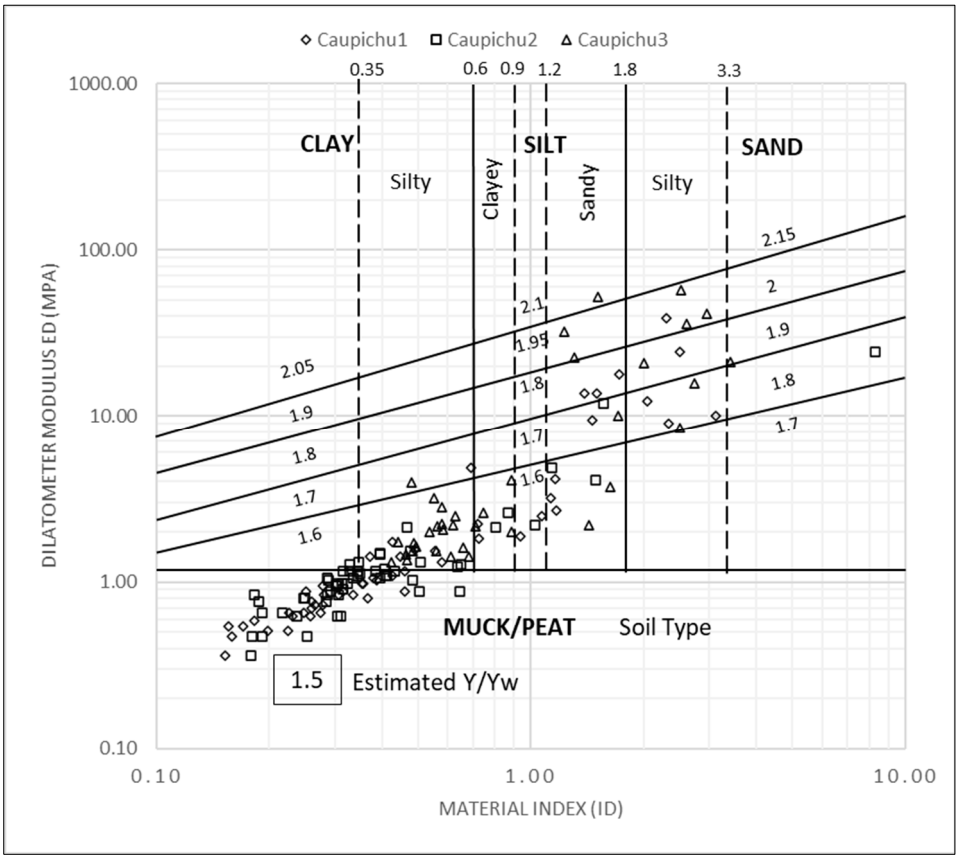

Figure 5. DMT results plotted on Marchetti's nomogram [36].

SDMT

The SDMT (seismic Marchetti's dilatometer test) is a combination of DMT equipment and a seismic module that measures the shear wave velocity Vs (Figure 6). Vs is obtained as the quotient of the source difference between two receivers spaced 0.5 m apart (S2–S1) and the pulse arrival delay from S1 to S2 (Δt) [37,38]. In Caupicho1, Vs measurements were obtained every 0.5 m of depth.

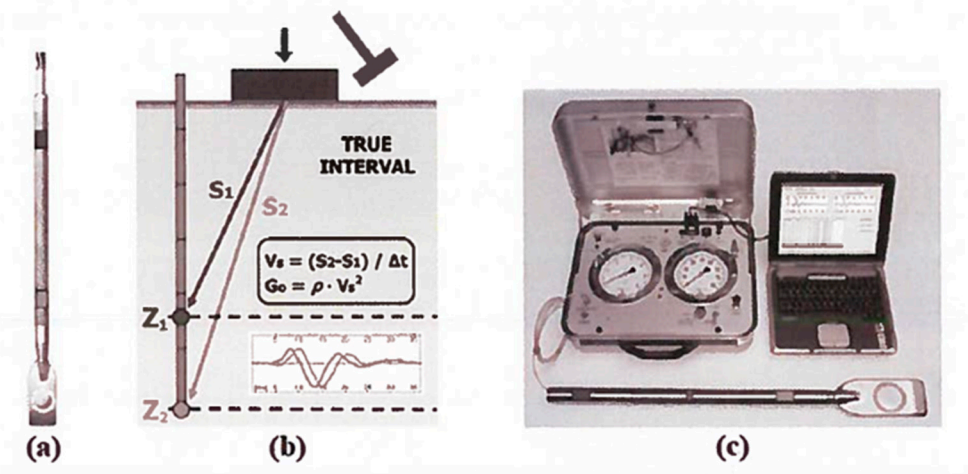

Figure 6. Materials and methods—seismic dilatometer: (**a**) DMT blade and seismic module; (**b**) schematic layout of the seismic dilatometer test; and (**c**) seismic dilatometer equipment [38].

Figure 7 shows three seismic wave velocity tests, Vs1, Vs2, and Vs3, obtained in Caupicho1 in relation to depth Z. On average, the results were as follows: 1.5–6.5 m: 74.3 m/s; 6.5–8.5 m: 330.3 m/s; 8.5–9.6 m: 82 m/s; and 9.6–10.5 m: 353.5 m/s.

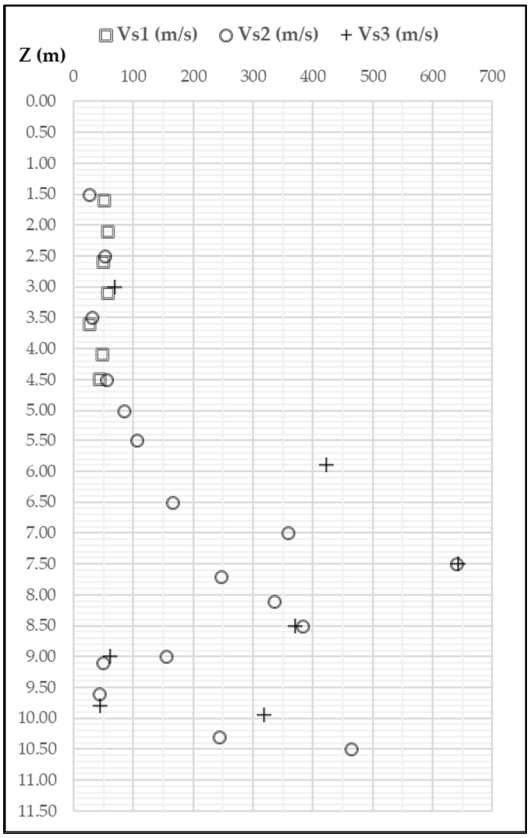

Figure 7. Results of three seismic wave velocity (Vs) tests for Caupicho1 [36].

Dissipation Test DMT-A

The DMT-A dissipation test (Figure 8) was performed at a depth of 5.30 m. The A readings were obtained at time intervals that were approximately doubled each time (15 s, 30 s, 1 min, 2 min, etc.). The A readings were plotted linearly against a logarithmic time scale, which describes the total pressure decay curve over time [39]. The data processing software used identified the inflection point Tflex = 1.81 min and estimated the consolidation coefficient Ch and permeability coefficient Kh using Equations (2)–(4), as listed in Table 11.

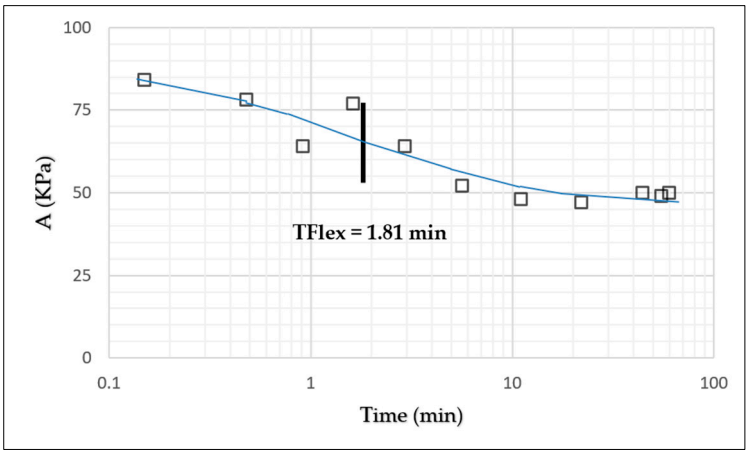

Figure 8. DMT-A dissipation test as a function of time.

$$Ch, DMTA \sim \frac{7\ cm^2}{Tflex} = \frac{7\ cm^2}{1.81\ min} \quad (2)$$

$$M_{DMT} = 0.14 + 2.36 log K_{D,}\ If\ I_D \leq 0.6 \quad (3)$$

$$Kh = \frac{Ch.Yw}{Ko.M_{DMT}} \quad (4)$$

Table 11. Marchetti's analysis. Calculation of horizontal permeability at depth Z.

Z (m)	K_D	Ko	M_{DMT}	Ch (cm²/min)	Kh (m/seg)
5.20	1.82	0.50	1.16	3.87	1.10×10^{-7}
5.40	1.87	0.51	0.51	3.87	2.42×10^{-7}

3.2. Laboratory Test Result

3.2.1. Mineralogical Analysis

Table 12 shows the petrographic analysis of a soil sample from Caupicho at a depth of 2.5 to 3 m.

Table 12. Petrographic mineralogical analysis of the Caupicho soil [24].

Petrographic Analysis (2.5–3 m)	%
Coalescence of cavities with clay mixture (CC)	2.00
Soil matrix (Matriz)	47.80
Pyroxenes (Px)	0.30
Plagioclases (Pl)	5.00
Organic material (RO)	23.40
Porosity	21.50
	100.00

Figure 9 shows an optical microscope image used in the mineralogical characterization, where GC represents the shrinkage cracks in the drying phase of the sample. The minerals present in the sample are of volcanic origin. The crystals present well-defined and angular shapes, suggesting little degree of transport [24].

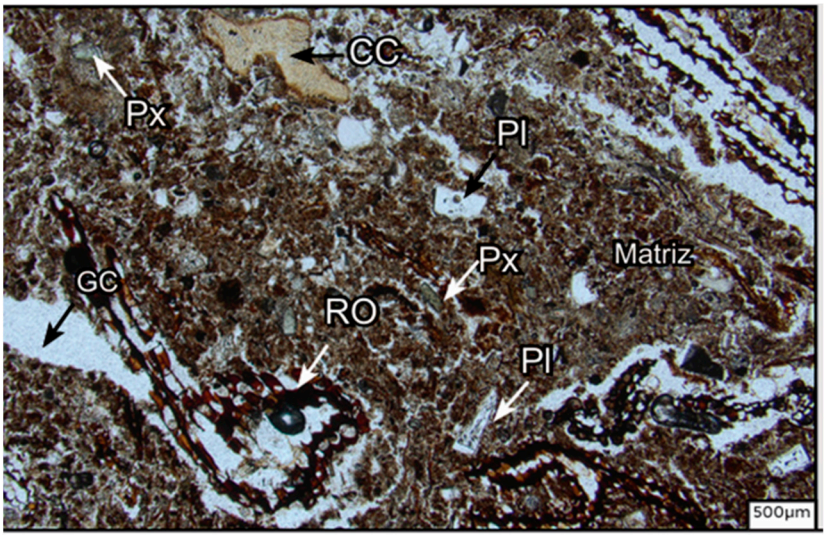

Figure 9. Microphotography of Caupicho soil. Department of Geology, Faculty of Geology and Petroleum, National Polytechnic School—Quito [24].

3.2.2. X-Ray Diffraction in Caupicho Soil

X-ray diffraction analysis was performed on the calcines obtained (61.1%). The results obtained from the X-ray diffraction analysis are detailed in Table 13 for a sample taken at a depth between 8.50 m and 9.00 m [25].

Table 13. Mineralogical analysis X-ray diffraction in Caupicho soil.

Mineral	Formula	Mineral Concentration (%)
Plagioclase	(Na,Ca) Al (Si,Al)Si_2O_8	78
Muscovite	$KAl_2(AlSi3O_{10})$ $(OH)_2$	17
Quartz	SiO_2	3
Cordierite	$Mg_2Al_4Si_5O_{18}$	2
		100

3.2.3. Scanning Electron Microscope (SEM)

The average elements obtained in 16 tests in six samples with depths from 2.50 m to 10.00 m are shown in Table 14.

Table 14. Analysis of chemical elements in Caupicho soil (2.50–10.00m) using SEM [26.].

Element	O	C	B	Si	N	Fe	Al	Na	Br	Ca	Ti	K	Mg	Total
Weight concentration (%)	41.02	33.46	11.59	5.25	3.03	2.84	1.01	0.55	0.53	0.39	0.16	0.10	0.07	100.00

Figure 10a–c show two twinned minerals A-B. Soil samples were obtained at depth of 4.50–5.00 m. Tables 15 and 16 show descriptions of the elements found at point 1 of the twinned minerals A-B.

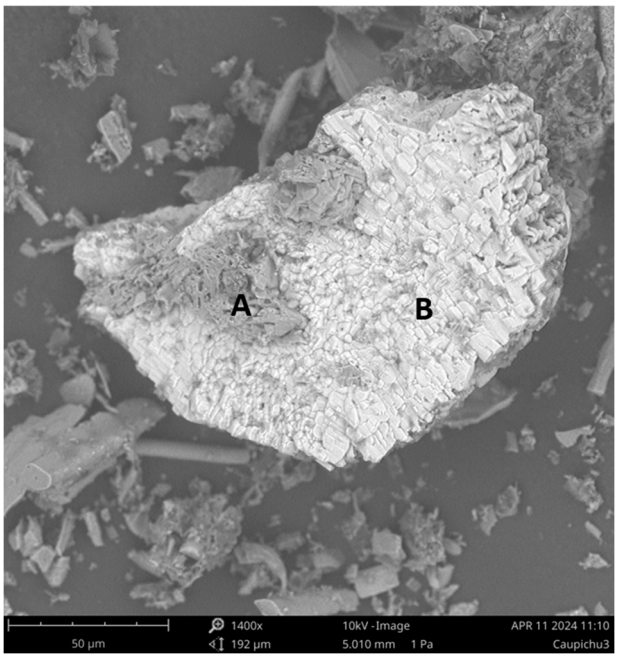

(**a**)

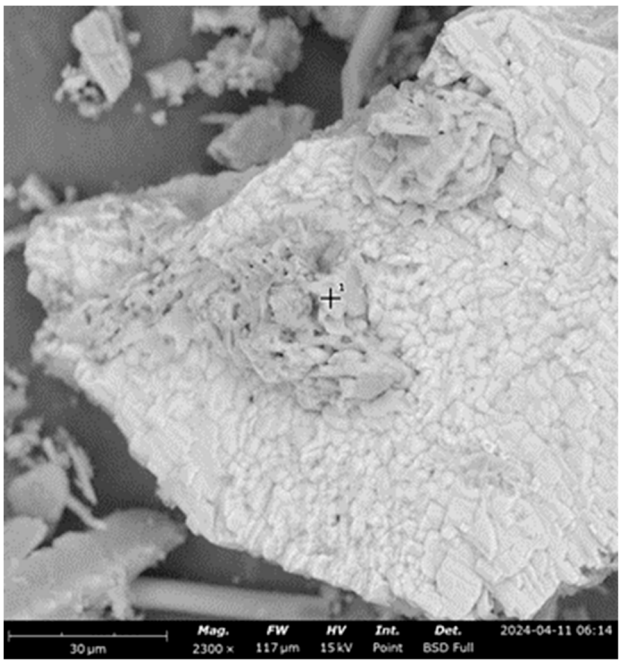

(**b**)

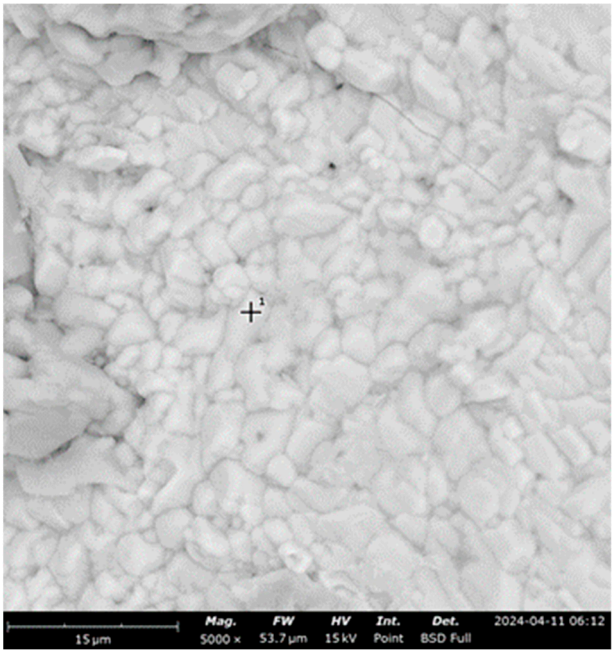

(**c**)

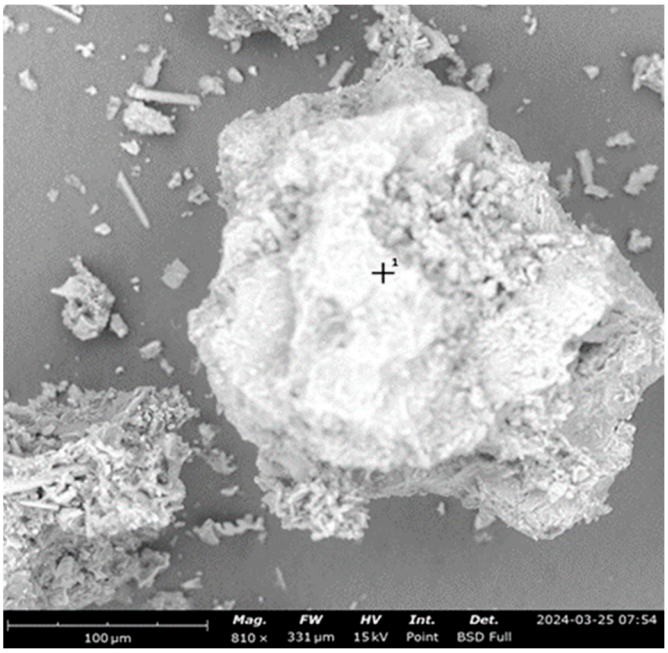

(**d**)

Figure 10. Morphology image Caupicho 4.50–5.00 m, listed as; (**a**) twinned mineral crystal; (**b**) point 1: evaluation of chemical elements in mineral A; (**c**) point 1: evaluation of chemical elements in mineral B. Morphology image Caupicho 9.50–10.00 m: listed as: (**d**) point 1: evaluation in soil particle.

Table 15. Analysis of the chemical elements in Caupicho at 4.50–5.00 m. Mineral A.

Element Number	Element Symbol	Element Name	Atomic Concentration (%)	Weight Concentration (%)
8	O	Oxygen	67.26	58.15
14	Si	Silicon	13.64	20.7
7	N	Nitrogen	10.92	8.27
13	Al	Aluminum	4.74	6.9
19	K	Potassium	1.96	4.15
11	Na	Sodium	1.48	1.83

Table 16. Analysis of chemical elements in Caupicho at 4.50–5.00 m. Mineral B.

Element Number	Element Symbol	Element Name	Atomic Concentration (%)	Weight Concentration (%)
6	C	Carbon	41.1	19.02
8	O	Oxygen	26.15	16.12
26	Fe	Iron	19.57	42.1
22	Ti	Titanium	11.15	20.56
14	Si	Silicon	2.03	2.2

Table 17 presents a description of the elements found at point 1 in the soil particles (Figure 10d). Soil samples were obtained at a depth of 9.50–10.00 m.

Table 17. Analysis of chemical elements from Caupicho at 9.50–10.00 m.

Element Number	Element Symbol	Element Name	Atomic Concentration (%)	Weight Concentration (%)
8	O	Oxygen	56.62	46.87
6	C	Carbon	23.59	14.66
14	Si	Silicon	12.45	18.1
35	Br	Bromine	3.16	13.07
11	Na	Sodium	1.79	2.13
26	Fe	Iron	0.86	2.47
20	Ca	Calcium	0.64	1.34
12	Mg	Magnesium	0.53	0.67

Microscopic fossils of diatoms have been found in the Caupicho soil at a depth of 4.50–5.00 m: unicellular algae with silica walls that developed in Andean lagoon environments mixed with allophanic volcanic ash (Figure 11), similar to soils found in Japan [40]

(**a**) (**b**)

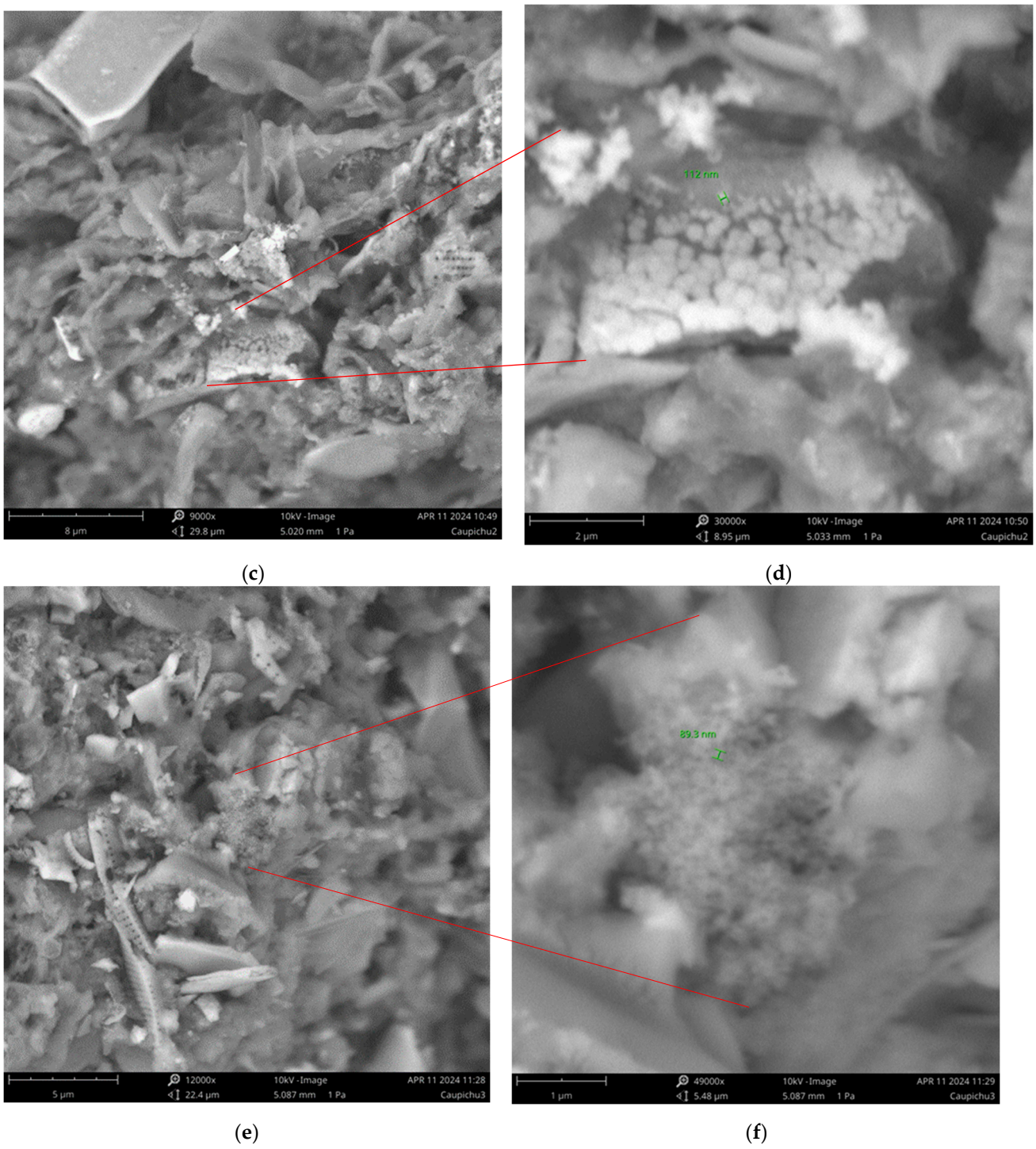

Figure 11. Morphology image Caupicho 4.50–5.00: (**a**) soil with diatoms; (**b**) set of diatoms with lengths of 5 to 10 µm; (**c**) soil, mineralization, and diatoms; (**d**) mineralization of approximate diameter 112 nm; (**e**) soil, allophane, and diatoms; and (**f**) allophane clusters < 89.3 nm.

3.2.4. Physical–Geotechnical Characterization

Figure 12 shows the physical–geotechnical parameters of Caupicho for altered and undisturbed samples with moisture contents between 100 and 350%, a liquid limit (Ll) between 100 and 325%, a plastic limit (Lp) between 50 and 200%, a soil classification SUCS - OH, a mineral content between 75 and 95%, and organic content between 5 and 25%.

A summary of the geotechnical–physical parameters of Caupicho for altered and unaltered samples from 1 to 10 m of depth is presented in Table 18.

Table 18. Summary of geotechnical physical characterization of the Caupicho soil.

Sample	Depth (m)	Natural Humidity (%)	LL (%)	LP (%)	IP (%)	Gross Sand (%)	Medium Sand (%)	Fine Sand (%)	Silt (%)	Clay (%)	SUCS	Ash Content (%)	Organic Content (%)	Gs (Li, 2020) †	Gs (Skempton & Petley, 1970) ‡
Altered	1.00–1.50	110.06	Insufficient sample			2.9	16.0	60.1	20.9	-		90.4	9.6	2.6	2.6
	2.00–2.50	217.77	225.0	181.4	43.6	0.3	1.8	19.5	78.4		OH	84.4	15.6	2.4	2.4
	3.00–3.50	233.74	213.3	186.0	27.4	0.0	0.7	19.5	79.8		OH	84.0	16.0	2.4	2.4
	4.00–4.50	302.95	226.8	181.5	45.1	0.0	1.4	19.5	78.8		OH	82.8	17.2	2.3	2.4
	5.00–5.50	320.38	310.9	180.5	130.4	0.3	3.9	13.9	63.0	18.9	OH	80.8	19.2	2.3	2.4
	6.00–6.50	316.36	326.0	200.5	125.8	0.0	3.4	15.6	63.9	17.0	OH	80.9	19.1	2.3	2.4
	7.00–7.50	107.5	98.1	77.6	20.5	0.1	0.5	21.0	78.4		OH	91.9	8.1	2.6	2.6
	8.00–8.50	200.41	165.5	105.9	59.6	0.0	0.8	20.8	69.5	8.9	OH	85.7	14.3	2.4	2.5
Unaltered Shelby	0.50–1.00	98.5	86.0	53.1	32.9	0.1	7.1	27.1	65.7		OH	92.8	7.2	2.6	2.6
	1.50–2.00	134.92	138.4	91.0	47.4	0.6	4.2	22.2	73.0		OH	95.1	4.9	2.6	2.7
	2.50–3.00	263.78	-	-	-	0.5	0.5	18.4	81.1	-		85.1	14.9	2.4	2.4
	3.50–4.00	238.99	225.3	159.6	65.7	0.1	0.5	16.2	73.2	10.0	OH	84.1	15.9	2.4	2.4
	4.50–5.00	320.7	317.0	186.7	130.4	0.0	0.8	15.0	67.2	17.0	OH	77.5	22.6	2.2	2.3
	5.50–6.00	341.9	-	-	-	-	-	-	-	-		78.4	21.6	2.3	2.3
	6.50–7.00	332.9	268.0	157.0	110.9	0.3	2.5	15.7	81.5		OH	74.0	26.0	2.2	2.2
	7.50–8.00	255.9	206.3	124.3	82.0	0.5	2.5	15.7	81.2		OH	89.2	10.8	2.5	2.5
	8.50–9.00	263.2	-	-	-	-	-	-	-	-		-	-	-	-
	9.50–10.00	353.5	145.9	104.5	41.4	0.7	7.8	21.9	51.7	18.0	OH	81.4	18.7	2.3	2.4

† [41], ‡ [42].

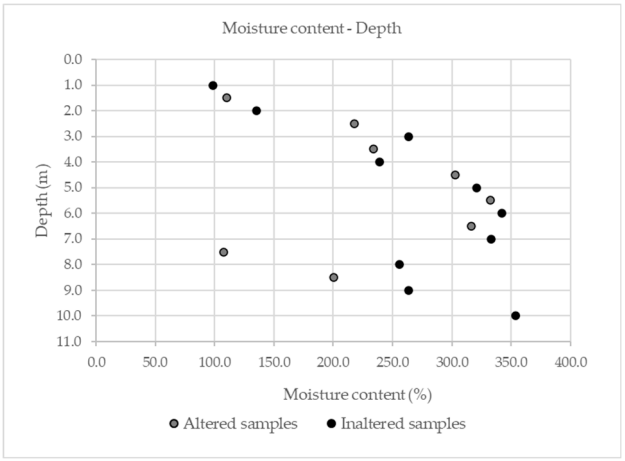
Moisture content - Depth
Depth (m)
Moisture content (%)
Altered samples
Inaltered samples

(**a**)

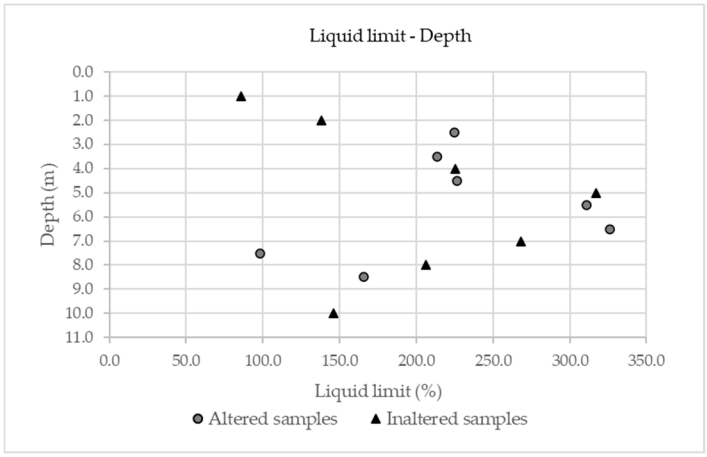
Liquid limit - Depth
Depth (m)
Liquid limit (%)
Altered samples
Inaltered samples

(**b**)

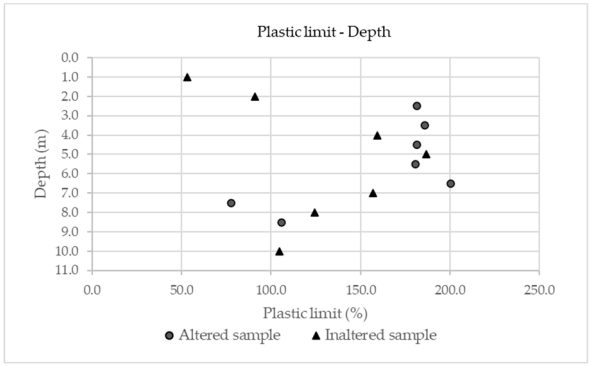
Plastic limit - Depth
Depth (m)
Plastic limit (%)
Altered sample
Inaltered sample

(**c**)

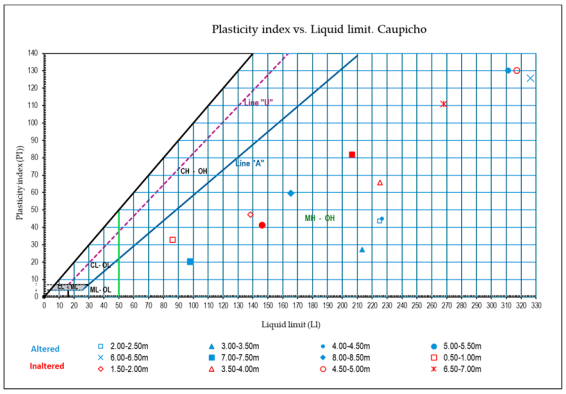
Plasticity index vs. Liquid limit. Caupicho
Plasticity index (PI)
Liquid limit (LL)
Line "U"
Line "A"
CH - OH
MH - OH
CL-OL
ML-DL
Altered
Inaltered
2.00-2.50m
3.00-3.50m
4.00-4.50m
5.00-5.50m
6.00-6.50m
7.00-7.50m
8.00-8.50m
0.50-1.00m
1.50-2.00m
3.50-4.00m
4.50-5.00m
6.50-7.00m

(**d**)

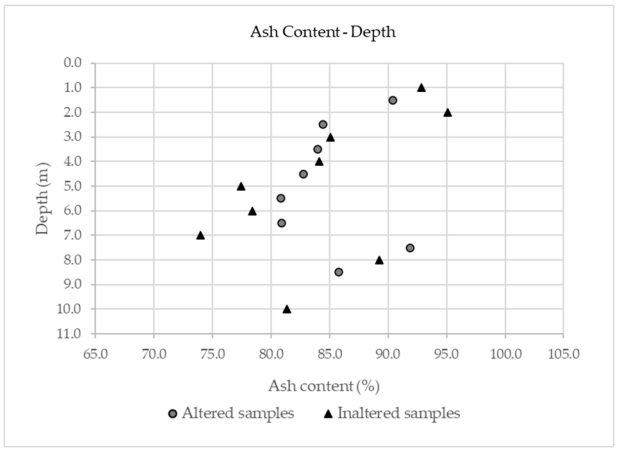
Ash Content - Depth
Depth (m)
Ash content (%)
Altered samples
Inaltered samples

(**e**)

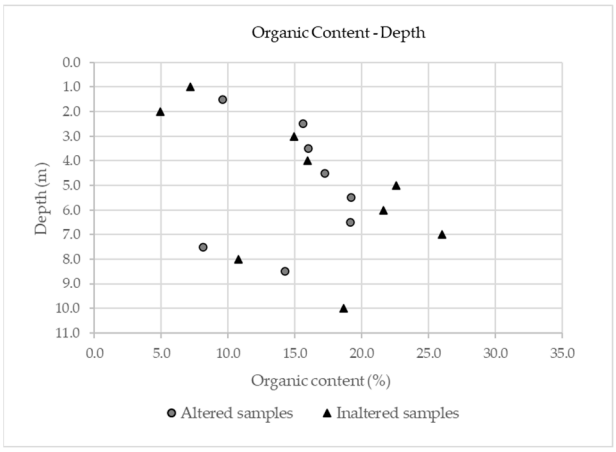
Organic Content - Depth
Depth (m)
Organic content (%)
Altered samples
Inaltered samples

(**f**)

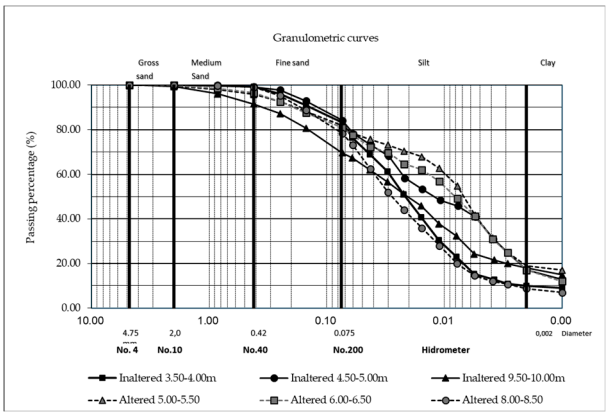

(**g**)

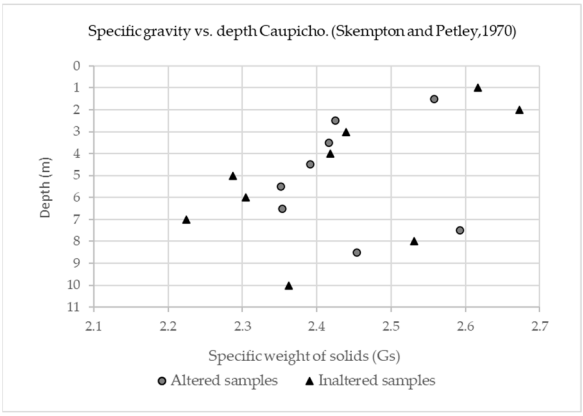

(**h**)

Figure 12. Geotechnical physical characterization of Caupicho as a function of depth: (**a**) moisture content; (**b**) liquid limit; (**c**) plastic limit; (**d**) plasticity index vsliquid limit; (**e**) ash content; (**f**) organic content; (**g**) altered and unaltered granulometric curves at different depths; and (**h**) specific weight of solids [42].

3.2.5. Mechanical–Geotechnical Characterization of Caupicho

a. Soil consolidation tests in Caupicho

Table 19 lists the laboratory soil parameters of the four samples used in the consolidation test.

Table 19. Initial data of the oedometric test for samples 1, 2, 3, and 4.

Sample	Depth	Particle Specific Gravity	Initial Moisture Content	Initial Bulk Density	Initial Dry Density	Initial Void Index (eo)	Initial Degree of Saturation	Porosity (n)
	m		%	Mg/m³	Mg/m³		%	%
1	6.5–7.0	2.24	288.46	1.07	0.28	6.92	90.85	87.50
2	2.5–3.0	2.27	257.16	1.14	0.32	6.14	95.14	85.90
3	5.5–6.0	2.18	366.79	1.04	0.22	8.79	91.01	89.91
4	8.5–9.0	2.24	256.54	1.15	0.32	5.93	96.86	85.71

The loading conditions for sample 1 were 12, 25, 50, and 100 Kpa, and the unloading pressures were 50, 25, and 12 MPa, respectively. For samples 2, 3, and 4, loading states of 25, 50, 100, 200, 400, and 800 with an average duration of eight days and unloading states of 200, 100, and 50 KPa with similar time averages were defined. Figure 13 shows the void index (e) as a function of the logarithm of pressure (log σ′) and logarithm of time (log t) for the four samples tested by consolidation.

Table 20 shows the results for the bulging index (Cs) and compression index (Cc).

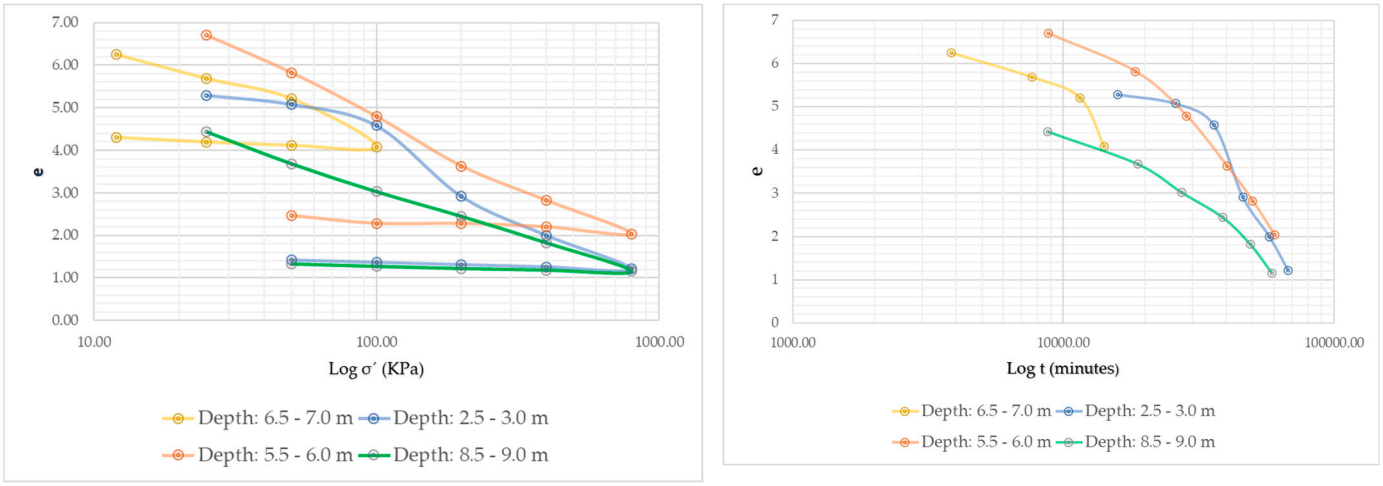

(**a**) (**b**)

Figure 13. (**a**) Void index (e) as a function of the logarithm of the effective pressure (log σ′), showing loading and unloading; (**b**) void index (e) as a function of the logarithm of time (log t) in minutes.

Table 20. Oedometric test calculations for samples 1, 2, 3 and 4.

Sample	Depth	Final Void Ratio (ef)	Final Degree of Saturation	Preconsolidation Pressure (σ′c)	σ′o	OCR (σ′c/σ′o)	Bulging Index	Compression Index
	m		%	Kpa	Kpa		Cs	Cc
1	6.5–7.0	4.32	99.75	25.00	19.09	1.31	0.23	3.71
2	2.5–3.0	1.44	99.72	20.00	18.84	1.06	0.18	2.65
3	5.5–6.0	2.42	99.10	22.40	20.84	1.07	0.35	2.57
4	8.5–9.0	1.31	99.77		28.68		0.15	2.21

Figure 14 shows the deformation curves in mm versus the root of time in minutes, as suggested by Taylor, 1942 [43].

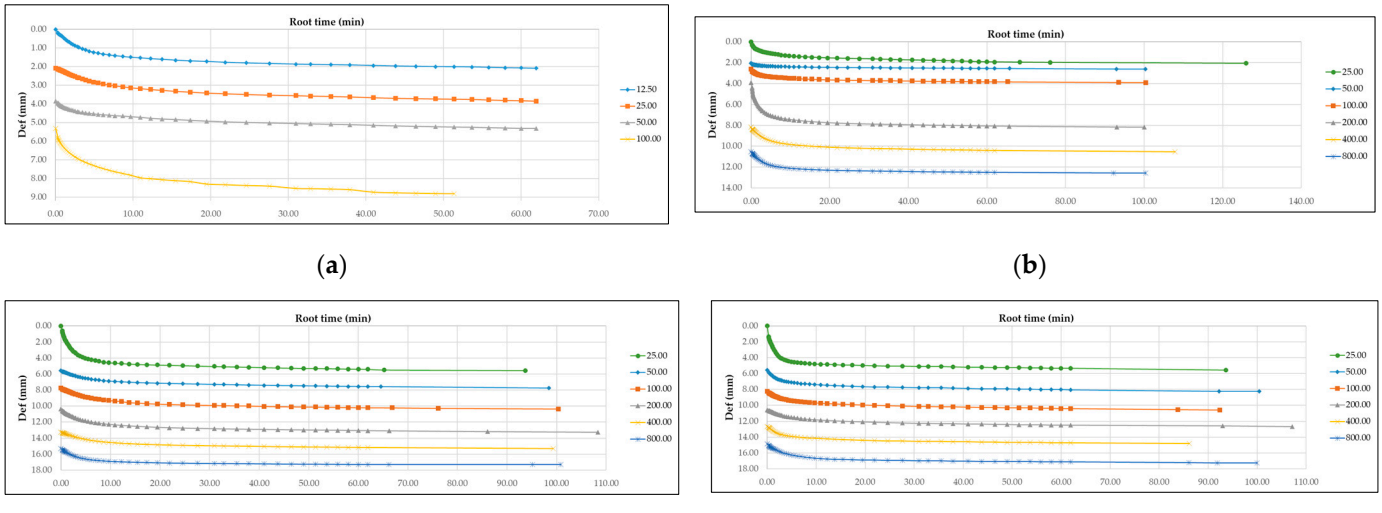

(**a**) (**b**)

(**c**) (**d**)

Figure 14. (**a**) Strain (mm) vs. root time (minutes) at different loads of 12.5, 25, 50, and 100 KPa for sample 1; (**b**) strain (mm) vs. root time (minutes) at different loads of 25, 50, 100, 200, 400, and 500 KPa for sample 2; (**c**) strain (mm) vs. root time (minutes) at different loads of 25, 50, 100, 200, 400, and 500 KPa for sample 3; (**d**) strain (mm) vs. root time (minutes) at different loads of 25, 50, 100, 200, 400, and 500 KPa for sample 4.

Table 21 shows the coefficient of consolidation (Cv) obtained using the Taylor method (1942) for sample 1.

Table 21. Coefficient of consolidation Cv at depth of 6.5–7 m from the oedometric test.

Pressure (Loading)	Coefficient of Consolidation (Cv)
Kpa	**mm²/min**
	Depth: 6.5–7.0 m
12.50	13.59
25.00	6.12
50.00	9.43
100.00	6.79

In Table 22, we present the coefficients of consolidation (Cv) obtained by the Taylor method (1942) for samples 2, 3, and 4.

Table 22. Coefficient of consolidation Cv at different depths of the oedometric test.

Pressure (Loading)	Coefficient of Consolidation (Cv)		
Kpa	**mm²/min**		
	Depth: 2.5–3.0 m	Depth: 5.5–6.0 m	Depth: 8.5–9.0 m
25.00	69.18	65.90	23.69
50.00	24.37	3.16	16.80
100.00	24.65	1.99	5.90
200.00	21.97	2.59	3.63
400.00	1.84	0.95	2.70
800.00	1.88	1.11	1.47

With the values of Cv, the specific gravity of water (Yw = 10 KPa), and the volume compressibility coefficient (mv) and using Formulas (5)–(7), we obtain the indirect permeability of the sample subjected to the consolidation test. Table 23 shows the average permeability for different effective stresses (σ′).

$$av = \frac{\Delta e}{\Delta \sigma'} \quad (5)$$

$$mv = \frac{av}{1 + eo} \quad (6)$$

$$k = Cv.\mathrm{Y}w.mv \quad (7)$$

Table 23. Vertical oedometric permeability analysis.

Sample	Depth	σ′	Kv = Cv.Yw.mv	σ′	Kv = Cv.Yw.mv	Kv Mean
	m	**Kpa**	**m/s**	**Kpa**	**m/s**	**m/s**
1	6.5–7.0	0–12	1.68×10^{-8}	12–25	6.36×10^{-9}	1.16×10^{-8}
2	2.5–3.0	0–25	5.53×10^{-8}	25–50	5.54×10^{-9}	3.04×10^{-8}
3	5.5–6.0	0–25	1.10×10^{-7}	25–50	2.55×10^{-9}	5.64×10^{-8}
4	8.5–9.0	0–25	3.98×10^{-8}	25–50	1.67×10^{-8}	2.82×10^{-8}
Kv average			5.55×10^{-8}		7.78×10^{-9}	3.16×10^{-8}

In Figure 15, we have permeability values of Kv = 1×10^{-7} m/s and 1×10^{-8} m/s for the initial loading phase and Kv = 1×10^{-9}–1×10^{-10} m/s for the further load increase in the consolidation test.

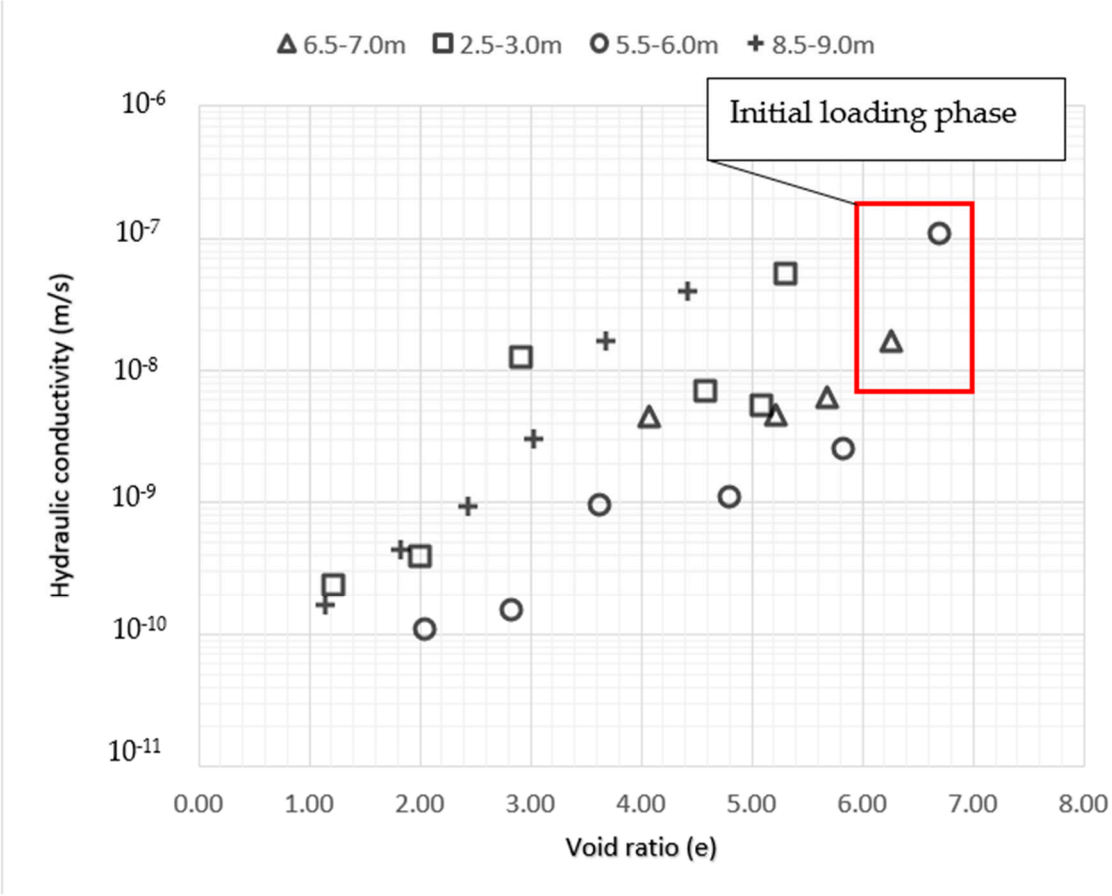

Figure 15. Hydraulic conductivity (Kv) as a function of void index at different depths in Caupicho1.

b. Drained consolidated triaxial test in the Caupicho (CD)

Table 24 shows the results of the consolidated–drained triaxial compression test on the cohesive soils of Caupicho. For axial deformations of 13.40–14.78%, effective friction angles ϕ′ = 25.5–30°, and effective cohesion c′ = 11.90–47.27 KPa.

Table 24. CD Triaxial–Caupicho1.

Depth (m)	Axial Strain (%)	ϕ′ (◦)	c′ (KPa)
2.5–4.0	14.75	30.00	16.67
4.0–5.0	14.74	25.49	20.90
5.0–6.0	13.40	30.05	47.27
6.5–8.0	14.78	28.74	11.90
Average	14.42	28.57	24.19

4. Discussion

4.1. In Situ Test Result

a. DMT Caupicho

Comparing Caupicho with Mayanquer, Albuja, and Seismic Quito, we have on average Cu = 5–15 Kpa, and in lower percentages, Cu = 20–40 Kpa; ϕ = 30–45◦; $Ko_{2\text{-}13\ m}$ = 0.5–0.7, far from average. In addition, P4-SQ $Ko_{1\text{-}11\ m}$ = 0.3–4; $OCR_{1\text{-}2\ m}$ = 1–13 (overconsolidated), $OCR_{2\text{-}4\ m}$ = 1–4, and $OCR_{4\text{-}13\ m}$ = 1 (normally consolidated); on average, Y = 13–16 KN/m^3, and in lower percentages, Y = 16–21 KN/m^3 (Figure 16).

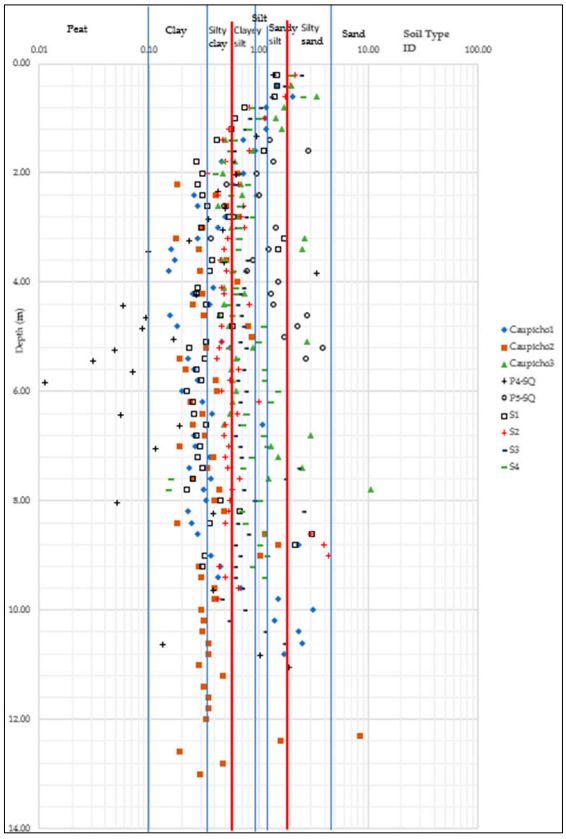
Peat
Clay
Silty clay
Clayey silt
Silt
Sandy silt
Silty sand
Sand
Soil Type ID
0.01
0.10
1.00
10.00
100.00
Depth (m)
0.00
2.00
4.00
6.00
8.00
10.00
12.00
14.00
Caupicho1
Caupicho2
Caupicho3
P4-SQ
P5-SQ
S1
S2
S3
S4

(**a**)

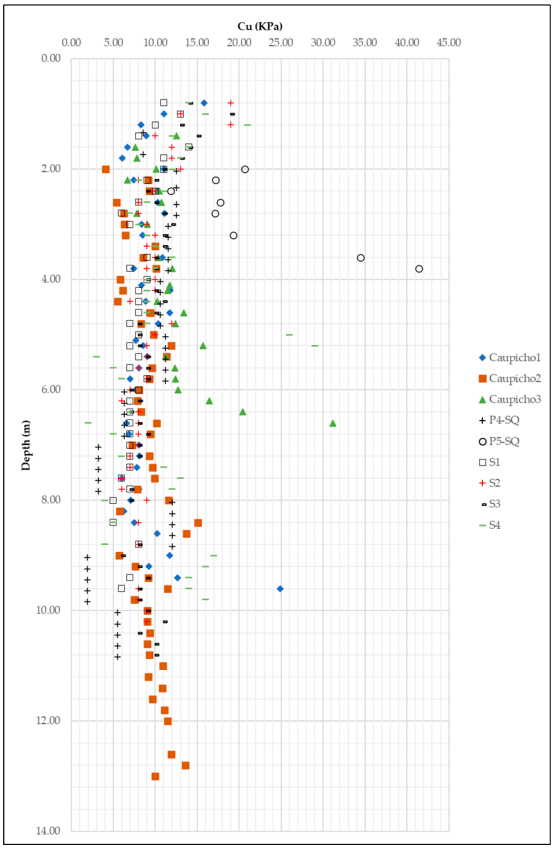
Cu (KPa)
0.00
5.00
10.00
15.00
20.00
25.00
30.00
35.00
40.00
45.00
Depth (m)
0.00
2.00
4.00
6.00
8.00
10.00
12.00
14.00
Caupicho1
Caupicho2
Caupicho3
P4-SQ
P5-SQ
S1
S2
S3
S4

(**b**)

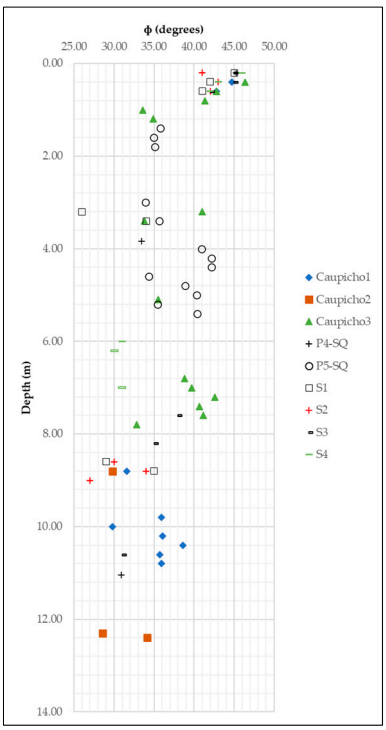
ϕ (degrees)
25.00
30.00
35.00
40.00
45.00
50.00
Depth (m)
0.00
2.00
4.00
6.00
8.00
10.00
12.00
14.00
Caupicho1
Caupicho2
Caupicho3
P4-SQ
P5-SQ
S1
S2
S3
S4

(**c**)

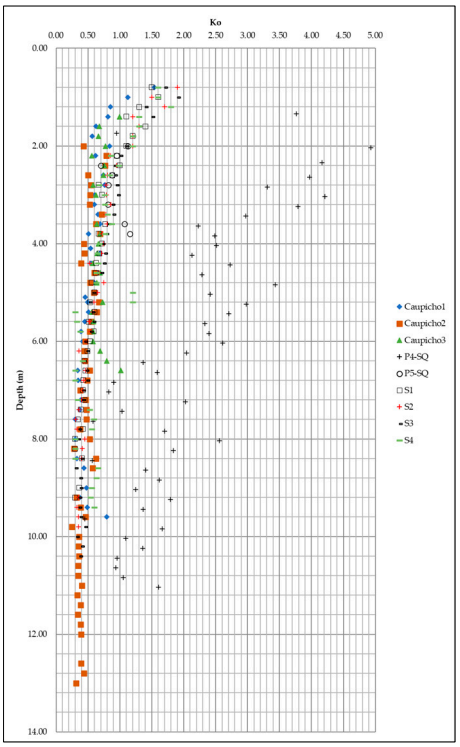
Ko
0.00
0.50
1.00
1.50
2.00
2.50
3.00
3.50
4.00
4.50
5.00
Depth (m)
0.00
2.00
4.00
6.00
8.00
10.00
12.00
14.00
Caupicho1
Caupicho2
Caupicho3
P4-SQ
P5-SQ
S1
S2
S3
S4

(**d**)

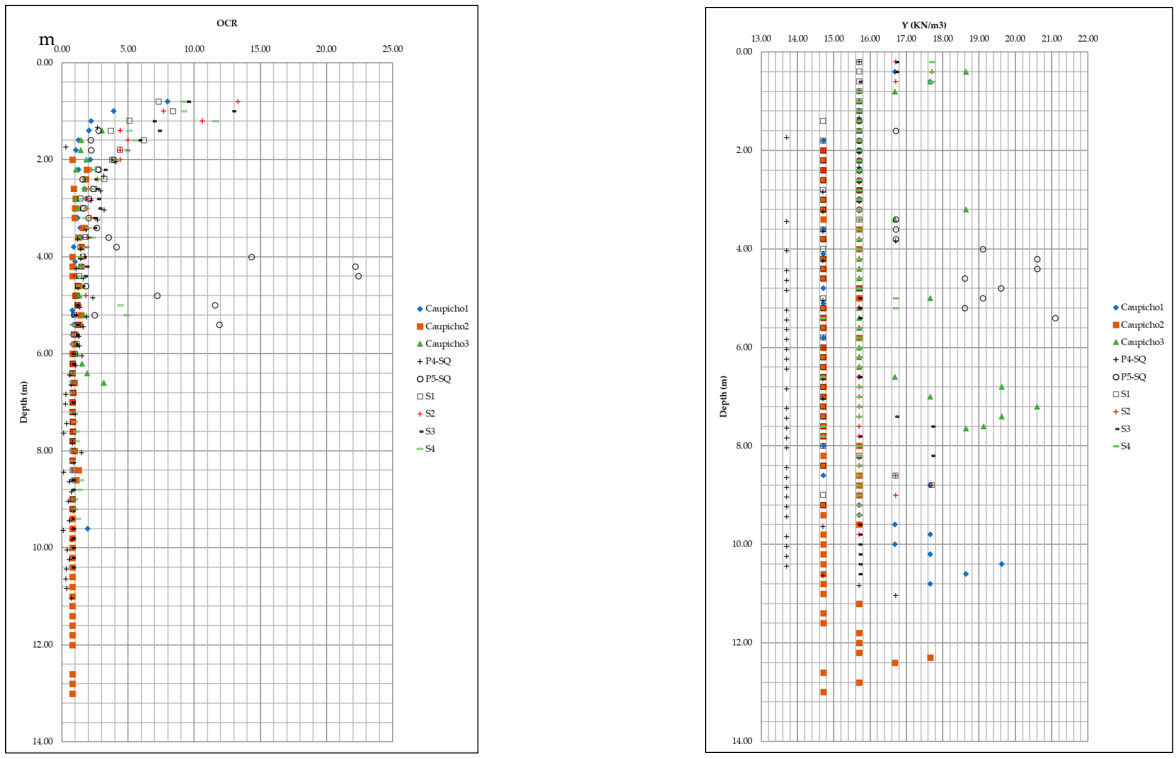

(**e**) (**f**)

Figure 16. Relation of Caupicho geotechnical parameters using the Marchetti dilatometer vs. Quito seismic zoning project (P4-SQ, P5-SQ) and Mayanquer (S1, S2, S3, S4), listed as: (**a**) material index (I_D)–depth; (**b**) cohesion of unconsolidated undrained soil (Cu)–depth; (**c**) angle of internal friction (ϕ) in degrees–depth; (**d**) coefficient of lateral soil pressure (Ko)–depth; (**e**) relationship between preconsolidation pressure σc and the present effective vertical pressure $\sigma'o$ (OCR)–depth; and (**f**) specific weight of soil (Y)–depth.

Comparing the Marchetti ID values in Table 25, we found a higher percentage of clays and silts and a lower percentage of sands. For P4-SQ, 34.48% of the soil was peat.

Table 25. Marchetti classification—type of soil per drilling: Caupicho, Mayanquer, Albuja, and Seismic Quito.

	Caupicho1			**Mayanquer**				**Albuja**	**Seismic Quito [6]**	
Soil	**1**	**2**	**3**	**S1**	**S2**	**S3**	**S4**		**P4-SQ**	**P5-SQ**
Peat	0.00	0.00	0.00	0.00	0.00	0.00	0.00	0.00	34.48	0.00
Clay	67.92	82.14	39.47	76.09	61.22	9.62	23.91	62.50	44.83	19.05
Silt	22.64	16.07	39.47	19.57	28.57	84.62	69.57	23.44	13.79	57.14
Sand	9.43	1.79	21.05	4.35	10.20	5.77	6.52	14.06	6.90	23.81
Total (%)	100.00	100.00	100.00	100.00	100.00	100.00	100.00	100.00	100.00	100.00

As seen in Table 26, Caupicho has 40.35% vs. Mayanquer's 21.08% of MUD (silt or clay mixed with water).

Table 27 shows a topographic difference of 22.92 between Caupicho3 and Mayanquer, which indicates that the soil deposits partially follow the original topography of the terrain.

Table 26. Marchetti classification—comparison of soil types between Caupicho and Mayanquer.

Soil	Caupicho	Mayanquer
MUD	40.35	21.08
Clay	20.09	22.17
Silt	23.60	45.59
Sand	15.96	11.15
Total (%)	100.00	100.00

Table 27. Topographic difference per study in meters above sea level.

Topographic Heigh		
Study	**Height z (m)**	**Δz**
Mayanquer	2994.46	22.92
Albuja	2993.73	22.19
Caupicho1	2986.39	14.85
Caupicho2	2976.18	4.64
Caupicho3	2971.54	0.00

b. SDMT–Vs Caupicho

Figure 17 shows the geographic location of the geophysical soundings. The information in Table 28 was obtained from nine shots per seismic line. The shot locations along the array were at −8.33 m (profile), 12.50 m, 29.17 m, 45.83 m, 62.5 m (center), 79.17 m, 95.83 m, 112.50 m, and 133.33 m (counter profile). Six hits were made at each position, resulting in 54 records per seismic line. Data processing was performed by the multichannel analysis of surface waves (MASW) method using the Geopsy software version 3.4.1 [44].

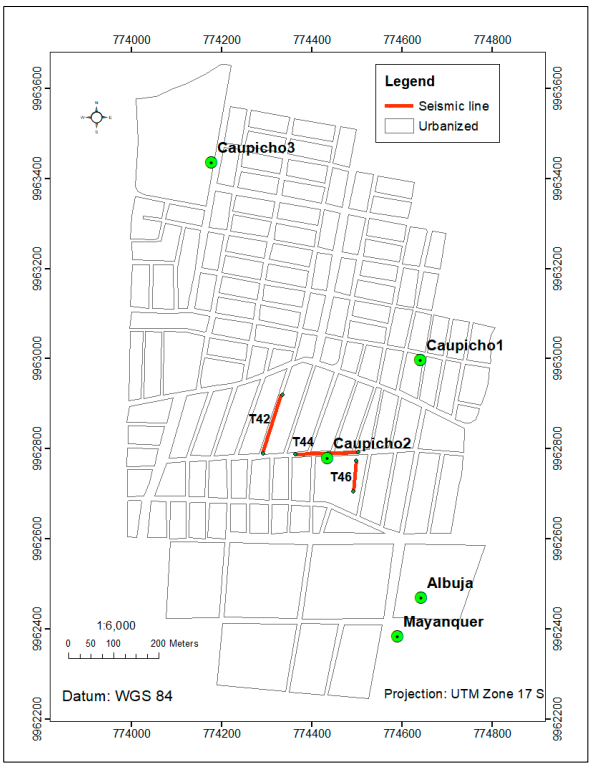

Figure 17. Geographical position of seismic traces: T42, T44, and T46.

To calculate Vs30, we used Formula (8):

$$Vs_{30} = \frac{\sum di}{\sum \frac{di}{Vs_i}} \quad (8)$$

In Table 29, we show the Vs values for Caupicho1 compared to the geophysical surveys T42, T44, and T46. It is observed that Caupicho1 has two strata of Vs: 74.30–82.00 m/s at depths of 1.50–6.50 m and 8.50–9.60 m, similar to the values obtained with CPTu in organic soil deposits [42]; two strata of Vs were observed: 330.25–353.50 m/s at depths of 6.50–8.50 m and 9.60–10.50 m. The geophysical borings T42, T44, and T46 present on average a Vs = 107.00 m/s for 60% of the borings and 120.00 m/s for 40% of the borings at a depth of 0.00–9.00 m, with a Vs = 239.00 m/s at maximum for a depth of 9.60–10.50 m.

In summary, Caupicho has Vs10 = 107–120 m/s and Vs30 = 169 m/s, with point strata showing Vs = 74–82 m/s and Vs = 330–354 m/s.

Table 28. Seismic wave velocity profiles Vs and Vs30 for geophysical surveys T42T44–T46 [44].

Shots	Layers	Depth (m)	d_i (m)	Vs (m/s)	Vs30 (m/s)	Depth (m)	d_i (m)	Vs (m/s)	Vs30 (m/s)	Depth (m)	d_i (m)	Vs (m/s)	Vs30 (m/s)
Profile	1	9.2	9.2	104.0	172.9	5.5	5.5	110.2	208.1	2.2	2.2	131.6	148.1
	2	15.6	6.4	250.0		15.2	9.7	236.7		19.5	7.3	157.4	
	3	17.7	2.2	105.8		17.6	2.4	177.0		26.2	6.7	104.9	
	4	30.0	12.3	314.2		30.0	12.4	312.4		30.0	3.8	315.0	
2-3	1	9.1	9.1	103.1	151.2	2.8	2.8	142.3	165.4	5.3	5.3	101.3	141.8
	2	20.9	11.7	193.0		18.9	9.7	151.2		14.0	8.7	200.2	
	3	24.7	3.9	120.0		18.9	6.4	103.1		27.2	13.3	123.6	
	4	30.0	5.3	312.4		30.0	11.1	311.5		30.0	2.8	312.4	
4-5	1	9.4	9.4	102.2	157.2	12.0	12.0	128.0	167.4	7.5	7.5	147.0	194.3
	2	19.0	9.6	201.9		14.2	13.0	157.4		11.0	3.5	206.4	
	3	23.0	4.1	137.8		20.8	6.6	114.7		16.7	5.7	191.2	
	4	30.0	7.0	315.0		30.0	9.2	312.4		30.0	13.3	315.0	
6-7	1	8.7	8.7	101.3	157.0	11.0	11.0	102.2	151.9	11.1	11.1	128.0	189.5
	2	11.5	2.8	196.6		15.0	4.0	229.5		12.5	1.4	185.0	
	3	17.8	6.3	123.6		19.0	4.0	105.8		15.0	2.5	157.4	
	4	30.0	12.2	305.2		30.0	11.1	315.0		30.0	15.0	312.4	
Center	1	11.6	11.6	104.9	146.6	7.1	7.1	101.3	176.9	5.0	5.0	118.2	149.0
	2	16.0	4.4	226.0		14.4	7.3	222.4		13.3	8.3	166.3	
	3	20.9	4.9	108.6		18.7	3.4	127.2		21.5	3.1	128.0	
	4	30.0	9.2	315.0		30.0	12.2	313.3		30.0	8.5	305.2	
10-11	1	4.6	4.6	105.8	190.0	9.7	9.7	101.3	171.3	3.7	3.7	109.3	148.5
	2	7.2	2.6	202.8		14.6	4.9	193.3		14.0	3.7	130.3	
	3	17.7	10.6	168.1		18.0	3.4	152.3		21.2	8.8	103.1	
	4	30.0	12.3	315.0		30.0	11.1	312.4		30.0	8.2	312.4	
12-13	1	6.8	6.8	103.1	193.1	4.6	4.6	108.4	180.6	3.7	3.7	103.1	150.6
	2	14.3	7.5	249.1		6.9	2.5	209.1		12.7	8.1	163.6	
	3	16.4	2.1	130.7		12.5	5.9	103.1		21.5	8.8	136.6	
	4	30.0	13.6	314.2		30.0	11.1	312.4		30.0	8.6	308.8	
14-15	1	9.0	9.0	102.2	175.3	1.1	1.1	108.4	178.9	8.4	8.4	144.9	176.0
	2	15.0	6.0	246.5		11.3	9.2	103.1		12.7	10.4	192.1	
	3	17.6	2.6	104.9		14.3	5.1	180.7		21.4	8.7	157.4	
	4	30.0	13.0	314.2		30.0	18.7	315.0		30.0	2.4	115.5	
Back Profile	1	10.8	10.8	102.2	166.4	9.1	9.1	100.4	162.4	2.4	2.4	115.5	182.7
	2	12.1	1.3	155.6		15.8	6.6	250.0		6.3	5.9	157.4	
	3	15.3	3.3	182.2		19.0	3.3	101.3		16.9	6.6	136.0	
	4	30.0	14.7	301.7		30.0	11.0	314.2		30.0	13.1	306.1	
Average Vs30 (m/s)					167.7				173.7				164.5

Table 29. Comparison of Vs between Caupicho and T42–T44–T46.

	Caupicho1	T42-T44-T46
Depth Z (m)	**Vs (m/s)**	
1.50–6.50	74.30	
6.50–8.50	330.25	107.00 (60%) 120.00 (40%)
8.50–9.60	82.00	
9.60–10.50	353.50	239.00 (max)

4.2. Laboratory Test

4.2.1. Mineralogical Analysis

The youngest domes of the Atacazo volcano with dacitic composition have been active for 12,000 years. The last activity corresponds to the Ninahuilca Chico II dome 2700 years ago [8]. Petrographic analysis and X-ray diffraction show minerals corresponding to andesite–dacite volcanic rocks; we observe a lower degree of weathering for the 2.5–3 m sample (Table 30) [45]. The Caupicho soils may have ages corresponding to the emissions from the Atacazo volcano. The well-defined and angular shapes of the minerals suggest volcanic deposits with little transport.

Table 30. Comparison of mineral characteristics of andesite and dacite with Caupicho.

Characteristic Minerals			**Degree of Weathering [45]**	**Minerals Found**	
	Andesite	**Dacite**		**Petrographic Analysis**	**X-Ray Diffraction**
				2.5–3.0 m	**8.5–9.0 m**
Quartz	X	X	1		X
Muscovite	X	X	2		X
Orthoclase		X	3		
Biotite	X	X	4		
Plagioclase	X	X	5	X	X
Amphibole	X	X	6		
Pyroxene	X		7	X	

4.2.2. Scanning Electron Microscope (SEM)

Allophane is an aluminosilicate consisting of a hollow unitary particle with a diameter of approximately 5.5 nm, with little or no structural organization. Electron micrographs show spongy aggregates with a rounded nodular appearance from weathered volcanic ash [46]. Figure 11e,f show spongy aggregates corresponding to the definition of an allophane formed in the material of lagoonal volcanic origin, with the presence of diatom fossils. SEM was used to identify the elements of inorganic and organic compounds (O, C, N, and B).

4.2.3. Geotechnical Physical Characterization

Figure 18a–c show a comparison between the moisture content, liquid limit, and plastic limit as a function of depth for Caupicho, Peñafiel, Albuja, and Mayanquer. Figure 18d shows a set of OH soil samples. Figure 18e,f show an average organic content of 12–24%. Figure 18g shows that silt predominates over sand and clay for Caupicho and Peñafiel. Figure 18h shows that the percentage of sand retained is 60–80% between Caupicho, Peñafiel, and Mayanquer. Figure 18i shows that the specific weight of solids (Gs) compared is between 2.1 and 2.7.

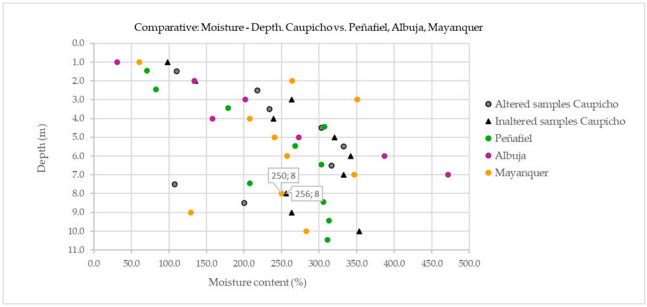
Comparative: Moisture - Depth. Caupicho vs. Peñafiel, Albuja, Mayanquer
Depth (m)
Moisture content (%)
250; 8
256; 8
Altered samples Caupicho
Inaltered samples Caupicho
Peñafiel
Albuja
Mayanquer

(**a**)

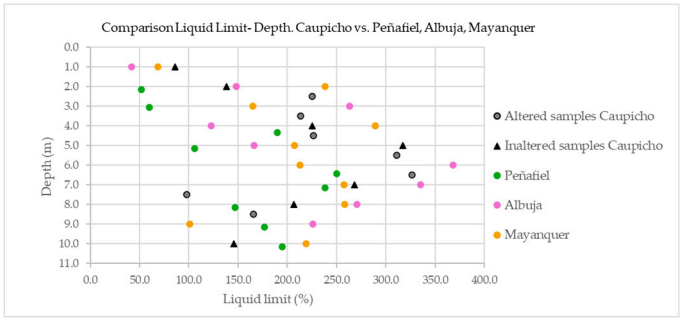
Comparison Liquid Limit- Depth. Caupicho vs. Peñafiel, Albuja, Mayanquer
Depth (m)
Liquid limit (%)
Altered samples Caupicho
Inaltered samples Caupicho
Peñafiel
Albuja
Mayanquer

(**b**)

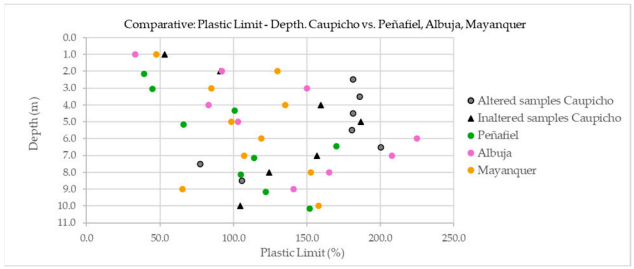
Comparative: Plastic Limit - Depth. Caupicho vs. Peñafiel, Albuja, Mayanquer
Depth (m)
Plastic Limit (%)
Altered samples Caupicho
Inaltered samples Caupicho
Peñafiel
Albuja
Mayanquer

(**c**)

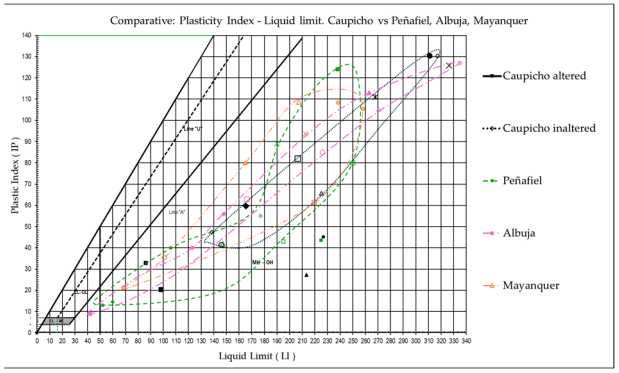
Comparative: Plasticity Index - Liquid limit. Caupicho vs Peñafiel, Albuja, Mayanquer
Plastic Index (IP)
Liquid Limit (LI)
Caupicho altered
Caupicho inaltered
Peñafiel
Albuja
Mayanquer

(**d**)

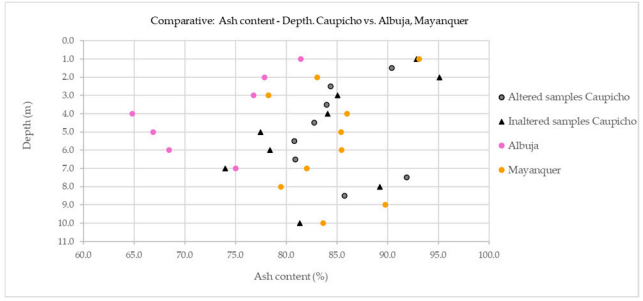
Comparative: Ash content - Depth. Caupicho vs. Albuja, Mayanquer
Depth (m)
Ash content (%)
Altered samples Caupicho
Inaltered samples Caupicho
Albuja
Mayanquer

(**e**)

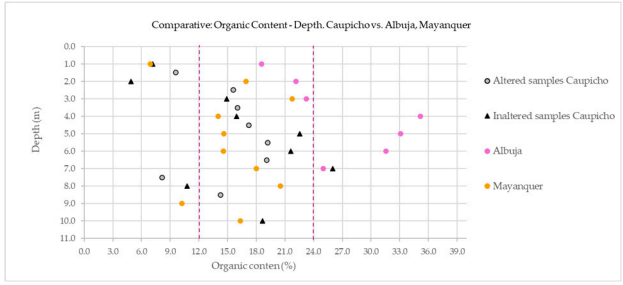
Comparative: Organic Content - Depth. Caupicho vs. Albuja, Mayanquer
Depth (m)
Organic conten (%)
Altered samples Caupicho
Inaltered samples Caupicho
Albuja
Mayanquer

(**f**)

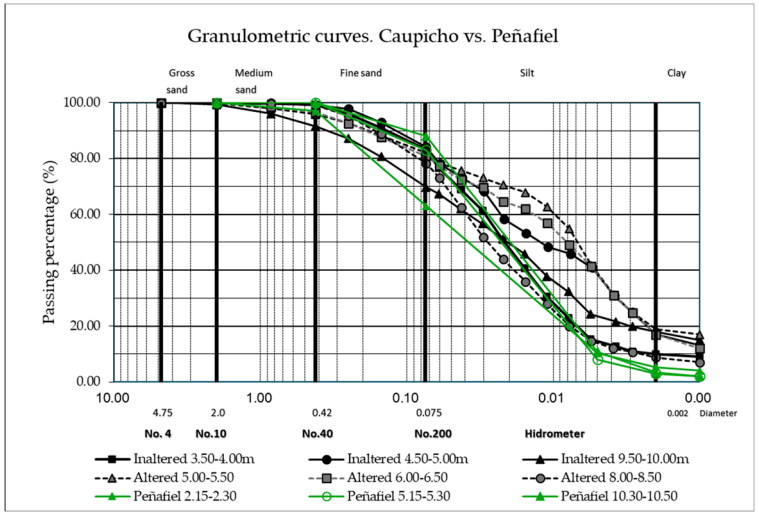

(**g**)

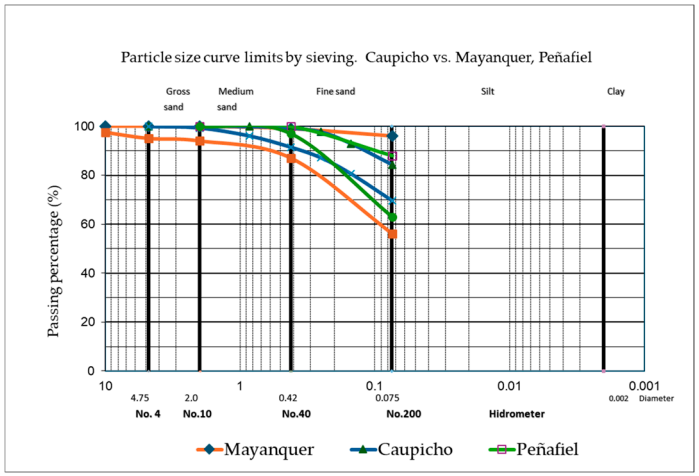

(**h**)

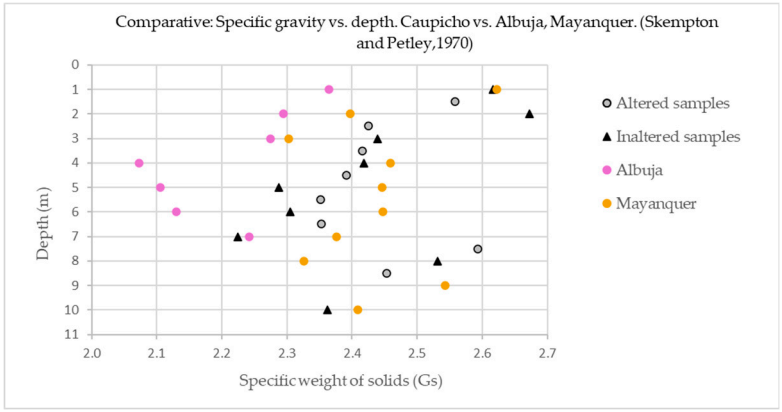

(**i**)

Figure 18. Relations of Caupicho with other geotechnical studies carried out previously in Peñafiel, Albuja, and Mayanquer [2–5] (See Figure 1), listed as: (**a**) humidity–depth; (**b**) liquid limit–depth; (**c**) plastic limit–depth; (**d**) comparative data set of liquid limit and plastic index; (**e**) ash content–depth; (**f**) organic content–depth; (**g**) granulometry curve limits by sieve and hydrometer; (**h**) granulometric curve limits by sieving; and (**i**) specific weight of solids (Gs)–depth [42].

Classifying the ash content found in Caupicho according to Figure 19 [13,14], the Caupicho soil is an organic mineral sediment which is non-peat.

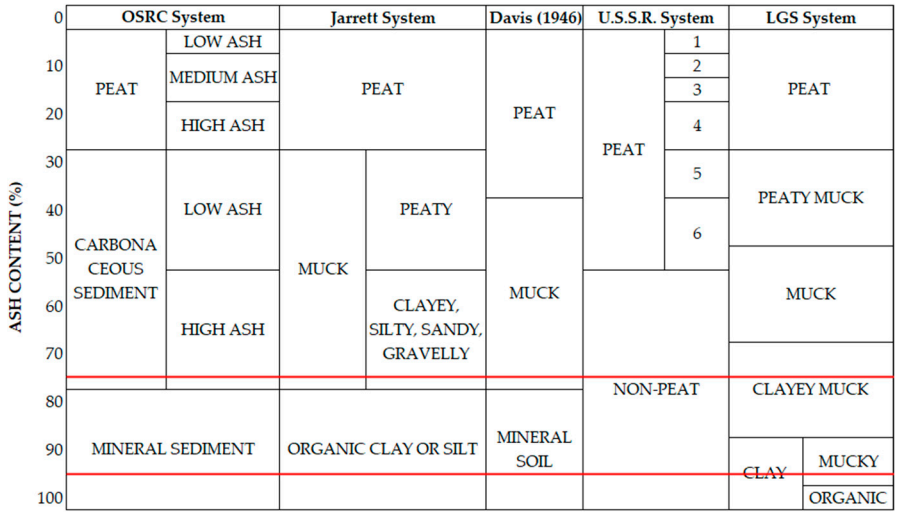

Figure 19. Comparison of soil classifications from different sources based on ash content [13,14].

4.2.4. Mechanical–Geotechnical Characterization

a. Soil consolidation test

Comparing the consolidation studies, Peñafiel had Cc = 0.95–3.16 [5], and Caupicho had Cc = 2.21–3.71. For a load of 25 KPa, Cv = 24–69 mm²/min, and the average is listed in Table 31.

Table 31. Coefficient of consolidation as a function of pressure and depth.

Depth	Pressure (Loading)	Coefficient of Consolidation (Cv)
m	KPa	mm²/min
2.5–3.0	50–800	14.94
5.5–6.0	50–800	1.96
8.5–9.0	50–800	7.45

In Table 32, we compare the results of the three peat studies with those of Caupicho. Levitico has a low amount of organics, as does Caupicho, and the Cs values for the four samples are in similar ranges. The Cc values were lower in Levitico than in Caupicho.

Table 32. Comparison of three different peaty soils (undisturbed or remodeled) with Caupicho in a one-dimensional consolidation test [47].

Sample	Levitico Peat	Fiavé Peat	Egna Peat	Caupicho
Mean specific gravity, Gs	2.3	1.8	1.6	2.2–2.3
Organic Specific weight Gsm	2.7	2.7	2.6	
Inorganic specific weight Gso	1.3	1.4	1.4	
Organic matter: %	19.9	49.3	71.0	5.0–26.0
Liquid limit, Wl: %	114.0	305.0	346.0	210.9
Plastic limit, Wp: %	76.0	183.0	226–272	142.1
Plastic index, Ip: %	38.0	126.0	121–74	68.8
Natural water content, w: %	150–180	209.0	280.0	245.9
Compression index, Cc Rem.	1.05–1.39	1.67		
Compression index, Cc Nat.	0.82	1.72	1.87	2.21–3.71

Swelling index, Cs Nat.	0.11–0.13	0.21		0.15–0.35
Swelling index, Cs Rem.	0.11	0.29	0.28	

In Figure 20 we compare e vs. log σ′, where we observe a greater variation in the void ratio when subjected to loads in the oedometric test in relation to a Fiave peat sample.

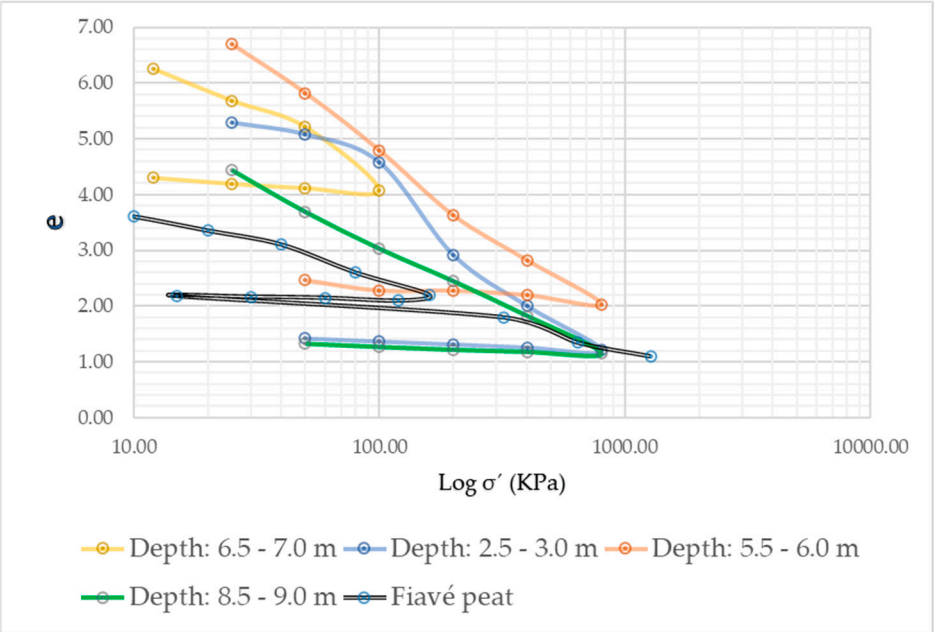

Figure 20. Relation of Caupicho with Fiavé peat, oedometric test [47].

b. Drained consolidated triaxial

In Table 33 we have a comparison of ϕ for different tests and soil types. Caupicho has values of the angle of internal friction of the drained consolidated triaxial test $\phi'C_D$ = 25.5–30°, lower than ϕ_{DMT} = 29–39°. The $\phi'C_D$ of Caupicho presents values comparable to those of other soils.

Table 33. Representative values for angle of internal friction ϕ′ vs. Caupicho.

	Type of Test			
	Unconsolidated Undrained	**Consolidated Undrained**	**Consolidated Drained**	**Reference**
Soil	**UU**	**CU**	**CD**	
Silt or silty sand				
Loose	20–22		27–30	[43]
Dense	25–30		30–35	"
Clay	0° if saturated	3–20°	20–42	"
Silty clay	17–22			[44]
Muddy	20.8			"
Peat			27.8–31.7 *	[45]
Organic silt–Caupicho			25.5–30 **	Current research

* Axial strain 20%; ** axial strain 14.4%.

The cohesion obtained in Caupicho by the Marchetti dilatometer test (DMT) ranges from 6.0 to 31.2 kPa, whereas the cohesion determined by the triaxial consolidated drained test (CD) was in the range of 11.9 to 47.3 kPa.

5. Conclusions and Recommendations

Structurally, to the east of the study area there is an anticlinal and geological fault parallel to the Machángara River. Petrographic analysis and X-ray diffraction show minerals corresponding to volcanic rocks, such as andesite–dacite, mainly from the volcanic emissions of Atacazo. The mineral crystals present well-defined and angular forms, suggesting a small degree of transport (volcanic ash). Electron micrographs show spongy aggregates with a rounded nodular appearance from the weathered volcanic ash (allophane). The Caupicho soil is an organic mineral sediment, with 57–70% silty muck, non-peat, and fossil diatoms, indicating a lacustrine period.

In Caupicho, we have an OH silt with organic content between 5 and 25%. The oedometric test gives us a compression index Cc = 2.21–3.71; swelling index Cs = 0.15–0.31; and consolidation coefficient Cv = 1.96–14.94 mm^2/min for pressure loads of 50–800 KPa. The drained consolidated triaxial test presents an effective friction angle $\phi' = 26–30°$ and effective cohesion c′ = 12–47 Kpa, with an axial deformation of 14%. The average soil permeability for effective stresses $\sigma' = 0–50$ KPa is $Kv = 3 \times 10^{-8}$ m/s (oedometer) and $Kh = 2 \times 10^{-7}$ m/s (DMT). The seismic wave velocities obtained are Vs = 74–82 m/s with two strata of 2 meters and 1 meter thick, with Vs values of 330 and 354 m/s respectively (DMT). The studies of Albuja, Peñafiel, and Mayanquer statistically coincided with the available geotechnical parameters of the soil, except for P4-SQ (Seismic Quito), which presented 35% peat according to the DMT test (I_D).

Cracks in the masonry of houses and enclosures indicate differential settlement due to consolidation in silt–organic muds limited by sand strata. Low-quality soil, seismic tectonic conditions, and accelerated urbanization in Caupicho should encourage new geotechnical studies on soil-bearing capacity, soil dynamics, and consolidation settlements.

Author Contributions: E.F.S.: investigation, conceptualization, and methodology; J.A.-S.: conceptualization, review, and supervision; M.C.: laboratory. All authors have read and agreed to the published version of the manuscript.

Funding: This study did not receive any external funding. Eddy Sanchez financed 60% of the project. The PUCE assumed the rest.

Institutional Review Board Statement: Not Applicable.

Informed Consent Statement: Not Applicable.

Data Availability Statement: The analyzed data can be provided upon request.

Acknowledgments: The authors would like to thank the Laboratory of Materials Strength, Soil Mechanics, Pavements, and Geotechnics, especially Jorge Erazo and Carlos Solorzano, and the staff of the Research Department of the Pontifical Catholic University of Ecuador (PUCE) for their support during the development of this research.

Conflicts of Interest: The authors declare no conflicts of interest.

References

1. Alvarado, A. Néotectonique et Cinématique de la Déformation Continentale en Equateur. Doctoral Dissertation, Université de Grenoble, Grenoble, Francia, 2012.
2. Mayanquer, J.; Anaguano-Marcillo, M.; Játiva, N.; Albuja-Sánchez, J. New Correlations for the Determination of Undrained Shear, Elastic Modulus, and Bulk Density Based on Dilatometer Tests (DMT) for Organic Soils in the South of Quito, Ecuador. *Appl. Sci.* **2023**, *13*, 8570. https://doi.org/10.3390/app13158570.
3. Albuja, J. Determination of the undrained shear strength of organic soils using the cone penetration test and Marchetti's flat dilatometer test. In Proceedings of the 6th International Conference on Geotechnical and Geophysical Site Characterization, Budapest, Hungary, 26–30 September 2021.

4. Albuja-Sanchez, J. Mechanical Properties of Peats. Submitted in fulfilment of the requirements for the MSc and the Diploma of Imperial College London, Imperial College London, London, UK, 2016.
5. Peñafiel, B.; Reascos, A. Caracterización Física, Geomecánica y Determinación de la Relación Entre el Índice de Plasticidad y el Coeficiente de Compresibilidad del Subsuelo del Sector "El Garrochal" Parroquia Turubamba. Pontificia Universidad Católica del Ecuador, Quito, Ecuador, 2021.
6. Albuja, J. Local Site Seismic Response in an Andean Valley: Geotechnical Characterization and Seismic Amplification Zonation of the Southern Quito Area. Universitá degli Studi di Ferrara, Ferrara, Italy, 2022.
7. Hidalgo, S.; Andrade, D. Presentación, Historia Volcánica. Actividad Actual, y Peligros Volcánicos Potenciales. Available online: https://www.igepn.edu.ec/publicaciones-para-la-comunidad/comunidad-espanol/tripticos/14156-triptico-volcanes-atacazo-ninahuilca-y-pululahua/file (accessed on 9 July 2024).
8. Hidalgo, S.; Monzier, M.; Almeida, E.; Chazot, G.; Eissen, J.-P.; Van Der Plicht, J.; Hall, M.L. Late Pleistocene and Holocene activity of the Atacazo–Ninahuilca Volcanic Complex (Ecuador). *J. Volcanol. Geotherm. Res.* **2008**, *176*, 16–26. https://doi.org/10.1016/j.jvolgeores.2008.05.017.
9. Panchana, C. Estudio de los Domos del Volcán Quilotoa y su Correlación con la Estratigrafía del Volcán. Escuela Politécnica Nacional, Quito, Ecuador, 2015.
10. Silva-Yumi, J.; Martínez, R.C.; Serrano, C.M.; Lescano, G.C. Alofán, Una Nanopartícula Natural Presente En Andisoles Del Ecuador, Propiedades Y Aplicaciones. *Granja. Rev. Cienc. Vida* **2021**, *33*, 53–66.
11. Mizota, C.; Carrasco, M.A.; Wada, K. Clay mineralogy and some chemical properties of Ap horizons of Ando soils used for paddy rice in Japan. *Geoderma* **1982**, *27*, 225–237. https://doi.org/10.1016/0016-7061(82)90032-5.
12. Guojun, L. Evaluation of Liquefaction Potential in Relation to the Shearing History Using Shear Wave Velocity. Doctoral Dissertation, Kyushu University, Fukuoka, Japan, 2019. https://doi.org/10.15017/2534440.
13. Andrejko. Michael; Fiene, F.; Cohen, A. Comparison of Ashing Techniques for Determination of the Inorganic Content of Peats. In *Testing of Peats and Organic Soils*; Jarret, P.M., Ed.; ASTM International: Toronto, ON, Canada, 1982.
14. Landva, A.O.; Korpijaakko, E.O.; Pheeney P. E. Geotechnical Classification of Peats and Organic Soils. In *Testing of Peats and Organic Soils*; Jarret, P.M., Ed.; ASTM International: Toronto, ON, Canada, 1982.
15. Arenaldi Perisic, G.; Ovalle, C.; Barrios, A. Compressibility and creep of a diatomaceous soil. *Eng. Geol.* **2019**, *258*, 105145. https://doi.org/10.1016/J.ENGGEO.2019.105145.
16. IGM. Instituto Geográfico Militar, Cartografía de Libre Acceso. Available online: https://www.geoportaligm.gob.ec/portal/index.php/descargas/cartografia-de-libre-acceso/ (accessed on 4 February 2024).
17. FAO. ClimWat. Land & Water Food and Agriculture Organization of the United Nations. Available online: https://www.fao.org/land-water/databases-and-software/climwat-for-cropwat/es/ (accessed on 20 February 2024).
18. FAO. CropWat. Land & Water Food and Agriculture Organization of the United Nations. Available online: https://www.fao.org/land-water/databases-and-software/cropwat/es/ (accessed on 20 February 2024).
19. MAG. Ministerio de Agricultura y Ganadería del Ecuador, (MAG). Available online: https://www.agricultura.gob.ec/ (accessed on 18 December 2023).
20. Aparicio, F. *Fundamentos de Hidrología de Superficie*; Limusa: México, México, 1999; ISBN 968-18-3014-8.
21. Guachamin, W.; García, F.; Arteaga, M.; Cadena, J. Determinación de Ecuaciones Para el Cálculo de Intensidades Máximas de Precipitación. Instituto Nacional de Meteorologia e Hidrologia (INAMHI). Ecuador. Available online: https://www.inamhi.gob.ec/Publicaciones/Hidrologia/ESTUDIO_DE_INTENSIDADES_V_FINAL.pdf (accessed on 15 July 2024).
22. *ASTM-D6635-15*; Standard Test Method for Performing the Flat Plate Dilatometer (Withdrawn 2024). Available online: https://www.astm.org/d6635-15.html (accessed on 18 March 2024).
23. Marchetti, S. In Situ Tests by Flat Dilatometer. *J. Geotech. Eng. Div.* **1980**, *106*, 299–321. https://doi.org/10.1061/AJGEB6.0000934.
24. Pilatasig, B. Análisis Mineralógico–Caupicho. Faculty of Geology and Petroleum, Department of Geology, National Polytechnic School, Quito, Ecuador, 2024.
25. Criollo, E.; Endara, D. Análisis de Difracción de Rayos x–Caupicho. Department of Extractive Metallurgy, National Polytechnic School, Quito, Ecuador, 2024.
26. Bolaños, D.; Espinoza-Montero, P. Análisis de Forma y Composición Química con Microscopio Electrónico SEM 400-800x. School of Chemical Sciences, Laboratory 007 of the Fundamental and Applied Electro-Chemistry Group GEFA, Pontificia Universidad Católica del Ecuador, Quito, Ecuador, 2024.

27. *ASTM D2216-19*; Standard Test Methods for Laboratory Determination of Water (Moisture) Content of Soil and Rock by Mass. Available online: https://www.astm.org/d2216-19.html (accessed on 17 August 2023).
28. *ASTM D4318-17*; Standard Test Methods for Liquid Limit, Plastic Limit, and Plasticity Index of Soils. Available online: https://www.astm.org/d4318-17e01.html (accessed on 17 August 2023).
29. *ASTM D1140*; Standard Test Methods for Amount of Material in Soils Finer than No. 200 (75-µm) Sieve. Available online: https://www.astm.org/d1140-00r06.html (accessed on 17 August 2023).
30. *ASTM D2487-17*; Standard Practice for Classification of Soils for Engineering Purposes (Unified Soil Classification System). Available online: https://www.astm.org/d2487-17.html (accessed on 18 August 2023).
31. *ASTM D2974-20*; Standard Test Methods for Determining the Water (Moisture) Content, Ash Content, and Organic Material of Peat and Other Organic Soils. Available online: https://www.astm.org/d2974-20e01.html (accessed on 12 September 2023).
32. *ASTM D7263-21*; Standard Test Methods for Laboratory Determination of Density and Unit Weight of Soil Specimens. Available online: https://www.astm.org/d7263-21.html (accessed on 12 September 2023).
33. *ASTM D4767-11*; Standard Test Method for Consolidated Undrained Triaxial Compression Test for Cohesive Soils. Available online: https://www.astm.org/d4767-11r20.html (accessed on 12 September 2023).
34. *ASTM D2435/D2435M*; Standard Test Methods for One-Dimensional Consolidation Properties of Soils Using Incremental Loading. Available online: https://www.astm.org/d2435_d2435m-11r20.html (accessed on 28 April 2024).
35. Rabarijoely, S. A New Approach to the Determination of Mineral and Organic Soil Types Based on Dilatometer Tests (DMT). *Appl. Sci.* **2018**, *8*, 2249. https://doi.org/10.3390/app8112249.
36. Marchetti, S.; Crapps, D. Flat Dilatometer Manual. Available online: https://www.marchetti-dmt.it/wp-content/uploads/bibliografia/marchetti_1981_crapps_manual.pdf (accessed on 16 July 2024).
37. Marchetti, S.; Marchetti, D.; Villalobos, F. El Dilatómetro Sísmico SDMT para ensayos de suelos in situ. *Obras Proy.* **2013**, 20–29. https://doi.org/10.4067/S0718-28132013000100002.
38. Marchetti, S.; Monaco, P.; Totani, G.; Marchetti, D. In Situ Tests by Seismic Dilatometer (SDMT). In *From Research to Practice in Geotechnical Engineering*; 2012; pp. 292–311. https://doi.org/10.1061/40962(325)7.
39. Marchetti, S.; Totani, G. Ch evaluations from DMTA dissipation curves. In *Congrès International de Mécanique des Sols et Des Travaux de Fondations*; 1989.
40. Gobin, M.; Yasufuku, N.; Liu, G.; Watanabe, M.; Ishikura, R. Small strain stiffness, microstructure and other characteristics of an allophanic volcanic ash. *Eng. Geol.* **2023**, *313*, 106967. https://doi.org/10.1016/J.ENGGEO.2022.106967.
41. Li, W.; O'Kelly, B.C.; Yang, M.; Fang, K.; Li, X.; Li, H. Briefing: Specific gravity of solids relationship with ignition loss for peaty soils. *Geotech. Res.* **2020**, *7*, 134–145. https://doi.org/10.1680/jgere.20.00019.
42. Skempton, A.W.; Petley, D.J. Ignition Loss and other Properties of Peats and Clays from Avonmouth, King's Lynn and Cranberry Moss. *Géotechnique* **1970**, *20*, 343–356. https://doi.org/10.1680/geot.1970.20.4.343.
43. Das, B.M. *Fundamentos de Ingeniería Geotécnica,* 4th ed.; Cengage Learning Editores, S.A., Ed.; México, 2015.
44. Mejía, R.; Mendoza, G. Aplicación del Método Geofísico MASW, Para la Obtención de Perfiles de Onda Vs y Cálculo de Vs30 del Subsuelo en la Microzonificación Sísmica del sur de Quito. Pontificia Universidad Católica del Ecuador, Quito, Ecuador, 2021.
45. Goldich, S.S. A Study in Rock-Weathering. *J. Geol.* **1938**, *46*, 17–58. https://doi.org/10.1086/624619.
46. Henmi, T.; Wada, K. Morphology and composition of allophane. *Am. Mineral.* **1976**, *61*, 379–390.
47. Madaschi, A.; Gajo, A. One-dimensional response of peaty soils subjected to a wide range of oedometric conditions. *Géotechnique* **2015**, *65*, 274–286. https://doi.org/10.1680/geot.14.P.144.